UNIVERSITA' DEGLI STUDI DI PADOVA
Dipartimento di Fisica e Astronomia
Dipartimento di Ingegneria Industriale

ISTITUTO NAZIONALE DI FISICA NUCLEARE
Laboratori Nazionali di Legnaro

Under the Auspice of the TESLA TECHNOLOGY COLLABORATION

MASTER THESIS
in
"Surface Treatments for Industrial Applications"

Development of a new mechanical surface treatment for the internal finishing of 6 GHz superconducting cavities

Supervisor: Prof. V. Palmieri
Co-Supervisor: Dott. A.A.Rossi

Student: Yu Guolong
N. Matr.: 1064843

Academic Year 2012-2013

有志者，事竟成。

Where there is a will, there is a way.

谨以此文献给我的妻子和儿子

二零一二年九月～二零一三年九月于意大利

Contents

CONTENTS .... **I**

ABSTRACT .... **V**

ACRONYM .... **VII**

CHAPTER 0 .... **1**

INTRODUCTION **1**

0.1 BACKGROUND AND PURPOSE 1
0.2 ORGANIZATION OF THE THESIS 1

CHAPTER 1 .... **3**

6 GHZ SPUN SEAMLESS CAVITIES **3**

1.1 TEV ENERGY SUPERCONDUCTING LINEAR ACCELERATOR (TESLA) CAVITIES 3
1.1.1 Key parameters and limitations *3*
1.1.2 Standard fabrication techniques [1] *5*
1.1.3 Disadvantages and limitation *7*
1.2 SEAMLESS CAVITIES 7
1.2.1 Description of Spinning technique *8*
1.2.2 RF measurements and results of seamless cavities *9*
1.3 6 GHZ CAVITIES 9
1.3.1 Advantages of 6 GHz cavities *10*
1.3.2 Drawback *11*
1.3.3 Standard surface polishing techniques *12*

CHAPTER 2 .... **15**

MECHANICAL POLISHING APPROACHES **15**

2.1 TURBULA® SHAKER-MIXER 15
2.2 CENTRIFUGAL BARREL POLISHING (CBP) 16
2.3 ZIGZAG TUMBLER 18
2.4 "FLOWER BRUSH" 19
2.4.1 "Flower brush" design for polishing 6 GHz cavities *19*
2.4.2 Polishing test *21*

CHAPTER 3 .... **25**

VIBRATING SYSTEM - A NEW MECHANICAL POLISHING APPROACH **25**

3.1 INDUSTRIAL APPLICATION OF VIBRATOR 25
3.2 RESONANCE-THE ORIGINAL IDEA 25
3.3 EXPERIMENT WITH SMALL VIBRATOR 27
3.3.1 The first experiment *27*

3.3.2 The second experiment *29*
3.4 VIBRATOR SYSTEM FOR 6 GHZ CAVITIES 30
3.4.1 Vibrator *31*
3.4.2 control box *31*
3.4.3 Mechanical configuration *34*
3.4.4 Falling detecting switch *36*

CHAPTER 4 .... **39**

AUTOMATION OF THE OPTICAL INSPECTION SYSTEM FOR 6 GHZ CAVITIES **39**

4.1 BEFORE UPDATING 39
4.1.1 System introduction *39*
4.1.2 The necessity of the automation *40*
4.2 THE REALIZATION OF AUTOMATION 41
4.2.1 Updating of mechanical part *41*
4.2.2 Design of Software *43*

CHAPTER 5 .... **48**

RESULTS **49**

5.1 MECHANICAL POLISHING PROCESS 49
5.1.1 Ultrasonic cleaning *49*
5.1.2 Media selecting *50*
5.1.3 Cavity polishing *50*
5.2 THE STATISTICS OF CAVITY TUMBLING 52
5.2.1 Different material cavities *52*
5.2.2 The highest erosion rate till now *53*
5.3 THE RF TEST RESULT 54
5.4 DISCUSSION 54
5.4.1 Effect of tumbling time *54*
5.4.2 Effect of media *55*
5.4.3 Single and multi-cavities tumbling *56*
5.4.4 Effect of plate direction *57*
5.5 SUMMERY 59

CHAPTER 6 .... **61**

CONCLUSIONS AND NEXT PLAN **61**

6.1 MECHANICAL POLISHING TREATMENT FOR 6GHZ CAVITIES 61
6.2 IDEA FOR 1.3GHZ MONO-CELL CAVITIES VIBRATION POLISHING SYSTEM 61

BIBLIOGRAPHY **63**

LIST OF FIGURES **65**

LIST OF TABLES **69**

ACKNOWLEDGEMENTS **71**

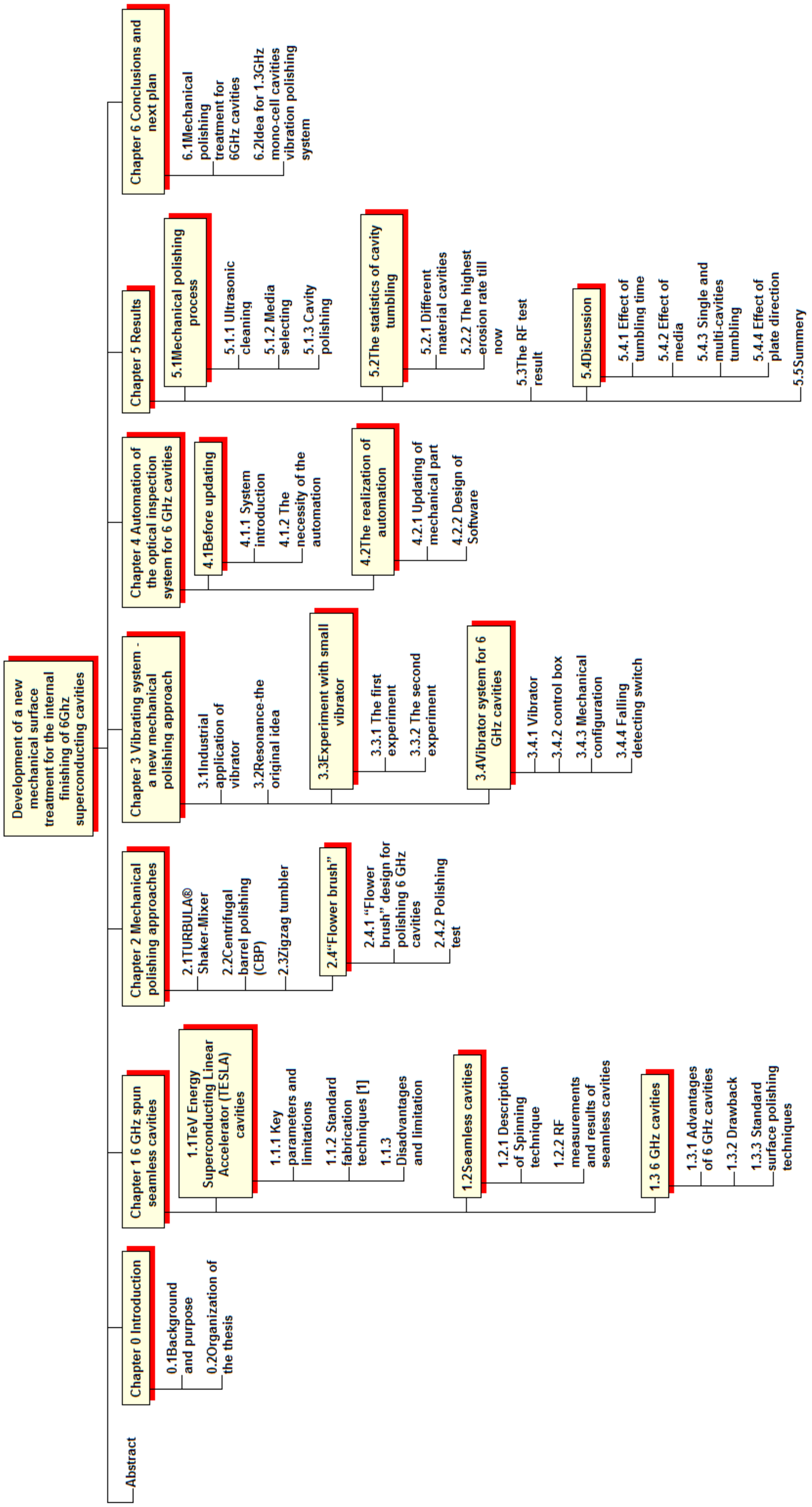
Development of a new mechanical surface treatment for the internal finishing of 6Ghz superconducting cavities
Abstract
Chapter 0 Introduction
0.1Background and purpose
0.2Organization of the thesis
Chapter 1 6 GHz spun seamless cavities
1.1TeV Energy Superconducting Linear Accelerator (TESLA) cavities
1.1.1 Key parameters and limitations
1.1.2 Standard fabrication techniques [1]
1.1.3 Disadvantages and limitation
1.2Seamless cavities
1.2.1 Description of Spinning technique
1.2.2 RF measurements and results of seamless cavities
1.3 6 GHz cavities
1.3.1 Advantages of 6 GHz cavities
1.3.2 Drawback
1.3.3 Standard surface polishing techniques
Chapter 2 Mechanical polishing approaches
2.1TURBULA® Shaker-Mixer
2.2Centrifugal barrel polishing (CBP)
2.3Zigzag tumbler
2.4"Flower brush"
2.4.1 "Flower brush" design for polishing 6 GHz cavities
2.4.2 Polishing test
Chapter 3 Vibrating system - a new mechanical polishing approach
3.1Industrial application of vibrator
3.2Resonance-the original idea
3.3Experiment with small vibrator
3.3.1 The first experiment
3.3.2 The second experiment
3.4Vibrator system for 6 GHz cavities
3.4.1 Vibrator
3.4.2 control box
3.4.3 Mechanical configuration
3.4.4 Falling detecting switch
Chapter 4 Automation of the optical inspection system for 6 GHz cavities
4.1Before updating
4.1.1 System introduction
4.1.2 The necessity of the automation
4.2The realization of automation
4.2.1 Updating of mechanical part
4.2.2 Design of Software
Chapter 5 Results
5.1Mechanical polishing process
5.1.1 Ultrasonic cleaning
5.1.2 Media selecting
5.1.3 Cavity polishing
5.2The statistics of cavity tumbling
5.2.1 Different material cavities
5.2.2 The highest erosion rate till now
5.3The RF test result
5.4Discussion
5.4.1 Effect of tumbling time
5.4.2 Effect of media
5.4.3 Single and multi-cavities tumbling
5.4.4 Effect of plate direction
5.5Summery
Chapter 6 Conclusions and next plan
6.1Mechanical polishing treatment for 6GHz cavities
6.2Idea for 1.3GHz mono-cell cavities vibration polishing system

Abstract

6 GHz spun seamless Superconducting Radio Frequency (SRF) cavities are a very useful tool for testing alternative surface treatments in the fabrication of TESLA cavity. However, the spinning technique has also some drawbacks like contamination, surface damage in internal part due to the collapsible mandrel line. The first important step of the surface treatments is the mechanical polishing. For this purpose, a new, cheap, easy and highly efficient tumbling approach based on vibration was developed.

Before this approach was conceived, a few other methods, such as Turbula, Centrifugal Barrel Polishing (CBP), custom Zigzag tumbler and “flower brush” have been studied and tested. But the result was not so satisfactory neither for the low erosion rate nor for the unstableness of the system nor for the complicated polishing process. At last, a vibration system with a simple structure, working stably was created after two experiments.

Another important task of the thesis is to update the optical inspection system for 6 GHz cavities. 3 stepper motors motor was added to move and rotate the cavity and realized auto focus of the miniature camera. A software was developed to achieve a full cavity photographed by one key operation using LabVIEW.

A high-efficiency mechanical polishing system is generally judged by two aspects: one is whether the surface property satisfies the demand after polishing; the other is whether the erosion rate can reach and be stabilized at a high value which is comparable or greater than the existing products. The Radio Frequency (RF) test result indicates that the vibration system is feasible. The latest erosion rate 1 gram/hour i.e. removing 13 microns depth of inner surface materials per hour exceeds the performance of CBP, which is widely used in other laboratories in the world.

The mechanical polishing process is elaborated and cavities that have been polished are listed. Several influencing factors on the erosion rate, such as tumbling time, media, signal and multi-cavities and plate direction are discussed at the end.

A preliminary design of 1.3 GHz vibration system as the future development is provided for the next plan.

Acronym

The acronyms used in this thesis are listed in the following,

ILC = International Linear Collider

INFN-LNL = Istituto Nazionale di Fisica Nucleare - Laboratori Nazionali di Legnaro (Padova)

TESLA = TeV Energy Superconducting Linear Accelerator

SRF = Superconducting Radio Frequency

RF = Radio Frequency

BCP = Buffered Chemical Polishing

CBP = Centrifugal Barrel Polishing

PCB = Printed Circuit Board

rpm = revolutions per minute

EB = Electron Beam

EP = Electro Polishing

HPR = High Pressure Water Rinsing

VFD = Variable-Frequency Drive

UHV = Ultra-High Vacuum

Chapter 0

Introduction

0.1 Background and purpose

Advantages of SRF cavities for accelerators are well known and a large number of 9-cells TESLA cavities is needed for the International Linear Collider (ILC). The fabrication of these cavities using the traditional way will cost much time and expensive. The spinning technology for seamless cavities invented in INFN-LNL is an answer for this challenge. Using this technology not only multi-cell 1.3 GHz resonators but also the 6 GHz cavity can be produced.

The mechanical polish for 6 GHz cavity is the first and important step, it will remove the defects and scratches of the inner surface due to using collapsible mandrel.

A high efficient mechanical treatment for the micro-cavities is a key to accelerate the process of studying the thin film deposition techniques and new superconducting materials for RF applications. The purpose of this thesis is to develop a new, cheap, easy and highly efficient tumbling approach.

0.2 Organization of the thesis

The first chapter introduces the origin of research. It gives a briefly introduction of TESLA cavities and the standard fabrication techniques, then expounds the seamless cavities technique, 6 GHz cavities and standard surface polishing techniques.

The second chapter describes the learning and trying of some mechanical polishing means for 6GHz resonator, including Turbula, Zigzag tumbler, CBP and polishing brush.

In chapter 3, the development of a new mechanical polishing approach and treatment is described in detail. It encompasses everything from birth of the ideas to the preliminary tests, from the working principle to the system structure.

Chapter 4 is an overview of the upgrading of cavity inner surface optical inspection system, involving both hardware and software, which is also an important part of this thesis.

The chapter 5 gives the results. It summarizes the mechanical polishing process, presents the statistics for the different materials cavity polished results, shows the highest polishing efficiency so far, states the RF test data, and finally discusses the impacts of abrasive materials type, quantity and mixing ratio, tumbling time, spatial arrangement of the vibrator on the polishing efficiency. It also compared the polishing efficiency of single cavity and multi-cavities in the same system.

The last part of the thesis is the conclusions and one idea for 1.3GHz mono-cell cavities vibration polishing system is proposed.

Chapter 1

6 GHz spun seamless cavities

1.1 TeV Energy Superconducting Linear Accelerator (TESLA) cavities

In the past 40 years, electron-positron collisions have played a central role in the discovery and detailed investigation of new elementary particles and their interactions. But some important fundamental questions still remain to be answered, which force the High Energy Physics community to build the next generation facility- the International Linear Collider (ILC) [1].

Superconducting radio-frequency (SRF) resonating cavity can operate in continuous-wave mode or long macro pulse mode, providing high acceleration gradients [2], therefore, it was chosen by the ILC.

The international TESLA project [3] uses nine-cell 1.3 GHz niobium cavities (shown in Figure 1.1), which reduce the cost per MeV by a factor of 20 over the then (year 1992) state-of-the-art SRF installation (CEBAF) by increasing the operating accelerating gradient by a factor of five from 5 MV/m to 25 MV/m, and reducing the cost per meter of the complete accelerating module by a factor of four for large-scale production [4].

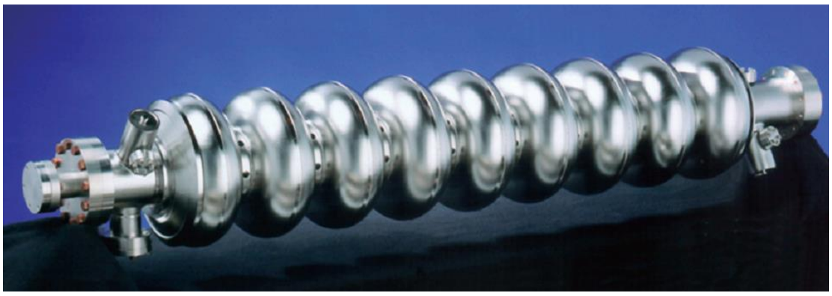

Figure 1.1 A TESLA nine-cell 1.3 GHz superconducting niobium cavity [4].

The TESLA 9-cell cavity is a standing wave structure of about 1 m length whose fundamental π -mode has a frequency of 1.3 GHz. It is made from 2.8mm thick high quality niobium sheets by deep drawing of half-cells, followed by trimming and electron beam welding.

1.1.1 Key parameters and limitations

- Surface resistance

There is an energy dissipation in superconductors in microware fields who penetrates a thin surface layer and induces oscillations of the electrons which are not bound in Cooper pairs. In the two-fluid model of superconductors one can derive an expression for the surface resistance

$$R_{BCS} = Ae^{-\frac{s}{2}\frac{T_c}{T}} \tag{1.1}$$

Here A is constant, s is strong coupling factor, approximate 3.8 for Niobium, is critical temperature, T is the bath temperature. In addition to the BCS term there is a residual resistance R_{res} caused by impurities (Figure 1.2), frozen-in magnetic flux, or lattice distortions. This term is temperature independent and amounts to a few nΩ for very pure niobium but may readily increase if the surface is contaminated.

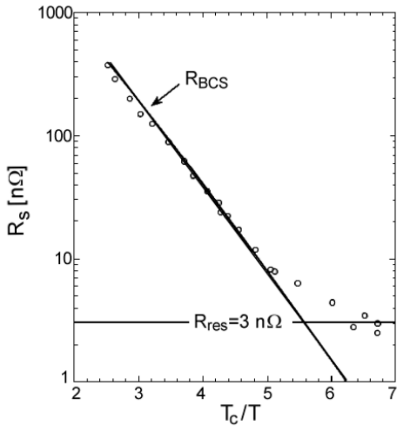

Figure 1.2 Measured surface resistance of a 9-cell TESLA cavity. The residual resistance of 3 nΩ corresponds to a quality factor of 10^{11}

The fundamental advantage of superconducting niobium cavities is the extremely low surface resistance of a few nano-ohms at 2 Kelvin as compared to several milli-ohms in copper cavities.

- Heat conduction in niobium

The heat produced at the inner surface of the cavity should be guided to the superfluid helium bath through the cavity wall. The thermal conductivity of the bulk Niobium and the temperature drop at the niobium-helium interface caused by the Kapitza resistance are two quantities that characterize the heat flow.

The RRR (residual resistivity ratio) value indirectly indicates the purity of the bulk metal as well as interstitial contamination that can affect the performance of the superconducting properties. An RRR value of 300 is considered desirable as its good thermal conductivity.

- Thermal instability and field emission

One basic limitation of the maximum field in a superconducting cavity is thermal instability. The heating by RF losses is not uniform over the whole surface but that certain spots where the defects locate exhibit larger temperature rises, often beyond the critical temperature of the superconductor. Hence the cavity becomes partially normal conducting, associated with strongly enhanced power dissipation. Because of the exponential increase of surface resistance with temperature, this may result in a runaway effect and eventually a quench of the entire cavity.

The tolerable defect size depends on the RRR of the material and the desired field level. As a typical number, the diameter of a normal-conducting spot must exceed 50 μm to be able to initiate a thermal instability at 25 MV/m for RRR>200 [5].

There have been many attempts to identify defects which were localized by temperature mapping. Examples of defects are drying spots, fibers from tissues, foreign material inclusions, weld splatter, and cracks in the welds. There are two obvious and successful methods for reducing the danger of thermal instability:

(i) avoid defects by preparing and cleaning the cavity surface with extreme care

(ii) increase the thermal conductivity of the superconductor.

Field emission of electrons from sharp tips is the most severe limitation in high-gradient superconducting cavities. In field-emission loaded cavities, the quality factor drops exponentially above a certain threshold and x rays are observed.

Small particles on the cavity surface (e.g., dust) is confirmed by the experimental that they act as field emitters [6]. Therefore, perfect cleaning, such as High-Pressure water Rinsing (HPR), is the most effective remedy against field emission. By applying this technique it has been possible to raise the threshold for field emission in multi-cell cavities from about 10 MV/m to more than 20 MV /m in the past few years.

1.1.2 Standard fabrication techniques [1]

The classic fabrication of a superconducting resonator consist of three major activities (see Figure 1.3[7])

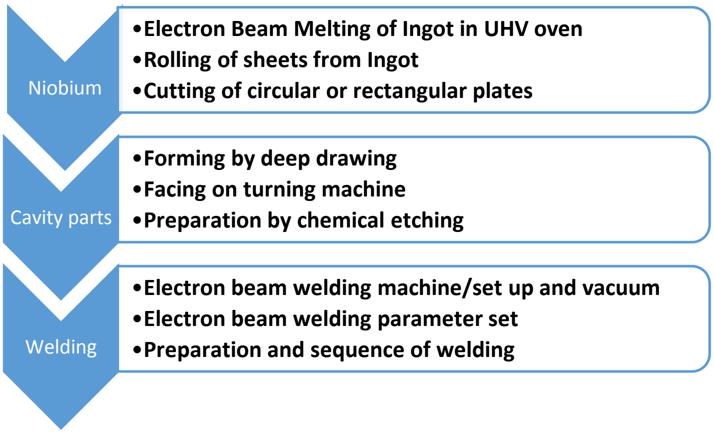

Figure 1.3 General fabrication steps of standard fabrication technique for s.c. Cavities

- Fabrication of Niobium

The 9-cell resonators are made from 2.8 mm thick sheet niobium by deep drawing of half-cells, followed by trimming and electron beam welding. Niobium of high purity is needed. Tantalum with a typical concentration of 500 ppm is the most important metallic impurity. Among the interstitially dissolved impurities, oxygen is dominant due to the high affinity of Nb for O_2 above 200℃. Interstitial atoms act as scattering centers for the unpaired electrons and reduce the RRR and the thermal conductivity. The niobium ingot is highly purified by several remelting steps in a high vacuum electron beam furnace. This procedure reduces the interstitial oxygen, nitrogen, and carbon contamination to a few ppm.

After forging and sheet rolling, the 2.8 mm thick Nb sheets are degreased, a 5 mm surface layer is removed by etching, and then the sheets are annealed for 1-2h at 700℃ -800℃ in a vacuum oven at a pressure of 10^{-5}-10^{-6} mbar to achieve full recrystallization and a uniform grain size of about 50 μm.

- Fabrication of Cavity parts and welding

Cups are produced by deep drawing. The dies are usually made from a high yield strength aluminum alloy. To achieve the small curvature required at the iris, an additional step of forming, e.g., coining, may be needed.

The half-cells are machined at the iris and the equator. At the iris the cup is cut to the specified length (allowing for weld shrinkage) while at the equator an extra length of 1 mm is left to retain the possibility of a precise length trimming of the dumbbell after frequency measurement. The accuracy of the shape is controlled by sandwiching the cups between two metal plates and measuring the resonance frequency. The cups are thoroughly cleaned by ultrasonic degreasing, 20mm chemical etching, and ultrapure water rinsing.

Two cups are then joined at the iris with an EB weld to form a “dumbbell.” The EB welding is usually done from the inside to ensure a smooth weld seam at the location of the highest electric field in the resonator. Since niobium is a strong getter material for oxygen, it is important to carry out the EB welds in a sufficiently good vacuum. Tests have shown that RRR=300 niobium is not degraded by welding at a pressure of less than 5×10^{-5} mbar.

The next step is the welding of the stiffening ring. Here the weld shrinkage may lead to a slight distortion of the cell shape which needs to be corrected. Afterwards, frequency measurements are made on the dumbbells to determine the correct amount of trimming at the equators. After proper cleaning by a 30mm etching, the dumbbells are visually inspected. Defects and foreign material imprints from previous fabrication steps are removed by grinding. After the inspection and proper cleaning (a few mm etching followed by ultraclean water rinsing and clean room drying), eight dumbbells and two beam-pipe sections with attached end cups are stacked in a precise fixture to carry out the equator welds which are done from the outside.

- Cavity treatment

The completed cavity has both internal and external chemistry to further remove the damage layer from the fabrication steps of both welding and handling. A smooth outer surface is necessary to provide good thermal contact with the cryogenic bath.

In total about 150-250 m of niobium material is removed from the interior RF surface of the cavity through several cleaning steps. After each of these acid etchings the cavity has a new superconducting RF surface and can have different RF performance and a different gradient limitation.

1.1.3 Disadvantages and limitation

The two primary issues with cavity fabrication are quality assurance on the niobium materials and on the electron beam welds. Niobium materials must be scanned to detect and eliminate surface defects, and then protected with care throughout the manufacturing process. Contaminated or defected material will ultimately limit the gradient performance of a completed cavity. As with the surface defects, impurities in the welds and heat a defected zones next to welds will also limit the gradient performance. Welds must have a smooth under bead and form no surface irregularities, in particular, sharp edges where the weld puddle meets the bulk material. Defects in the equator welds will limit the gradient by thermal quenches due to the high magnetic fields there. Thermal mapping of quench locations suggests that they are typically located at or near the equator region.

Cavity fabrication by electron-beam welding of deep-drawn half-cells is a delicate procedure [5], requiring intermediate cleaning steps and a careful choice of the weld parameters to achieve full penetration of the joints. First, two half cells are connected at the iris; the stiffening rings are welded in next. At this point weld shrinkage may lead to a slight distortion of the cell shape which needs to be corrected. Particularly critical are the equator welds, which are made from the outside, and a reliable method for obtaining a smooth weld seam at the inner cavity surface was required.

1.2 Seamless cavities

20,000 nine-cell resonators would be required for the ILC [4]. A great many physicists believe that a so huge amount of resonators could be manufacturable using the standard fabrication technique [8], and the bare bulk Niobium cavity costs roughly include material costs and fabrication costs. 500 tons of high purity Niobium will be need; the procedure of EB welding is very complicated as described in the previous section and longtime costs. For this reason there is a trend to research on alternative fabrication technology [9]

At the National Institute of Nuclear Physics in Legnaro (INFN-LNL) the well-known spinning technique has been adapted to form a fully seamless resonator without electron beam welding [13]. In this way, starting from a disk or a seamless tube, it is possible to build seamless cavities with no intermediate annealing, more rapidly, simply, and with a uniform thickness. Both 1.3 GHz niobium and copper cavities can be easily manufactured with high reproducibility and significant savings in manufacture costs.

1.2.1 Description of Spinning technique

Spinning of a seamless mono-cell resonator from a circular blank is depicted on Figure 1.4. The process is mainly divided in four steps [10]. A circular disk of 400 mm diameter and 3 mm thickness is first preformed onto a frustum shaped mandrel, then the first half-cell is formed and a cylindrical shape is given to the remaining part of the piece, by means of a second pre-mandrel. The third step consists in spinning the obtained manufacture onto a collapsible mandrel that has exactly the same shape of the cavity interior, up to when the roller overcomes the equator and fixes the piece to spin onto the mandrel. Then the fourth and last step consists in inserting a further frustum-shaped collapsible mandrel in order to guide the material when spinning the second half-cell. Both collapsible mandrels are then removed.

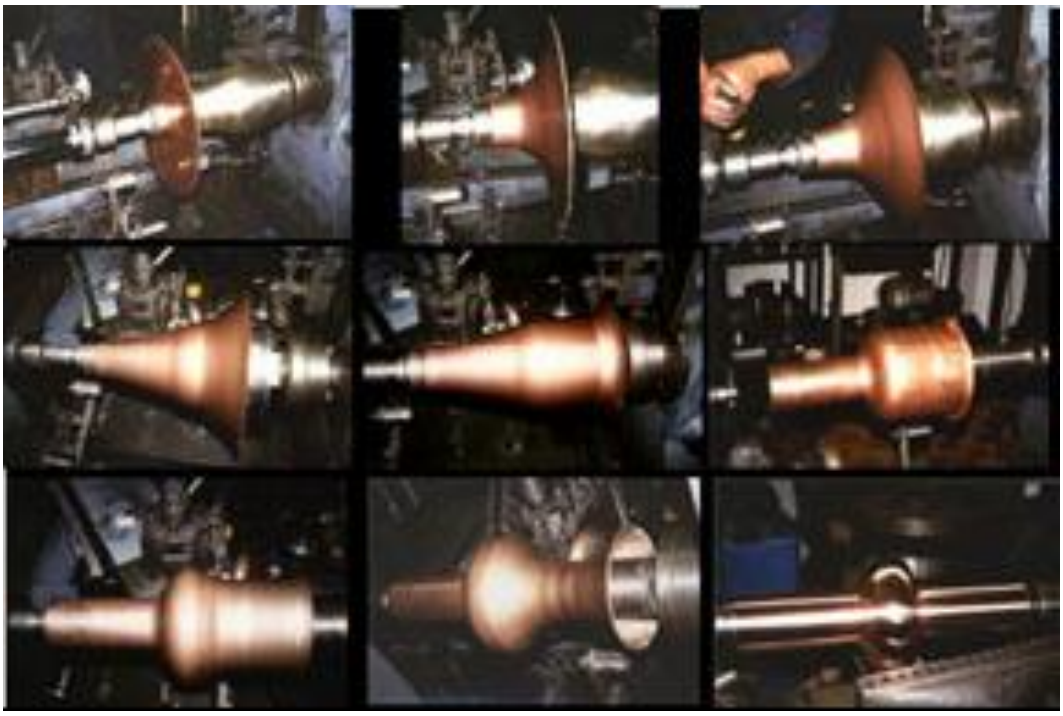

Figure 1.4 Spinning of a seamless mono-cell resonator from a circular blank. No intermediate annealing is required during forming.

Figure 1.5 shows schematically the various manufacturing steps needed for conventional cavity fabrication and the reduced number of manufacturing steps for fabrication of seamless cavities.

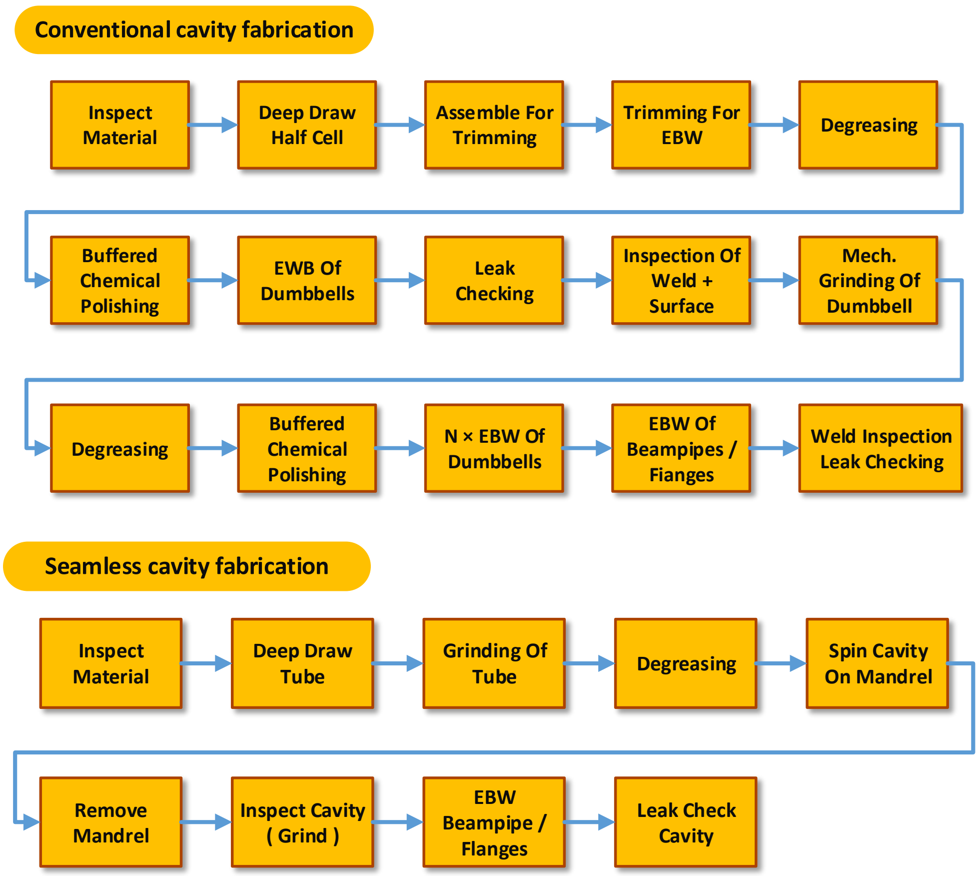

Figure 1.5 Process comparison of conventional and seamless cavity Fabrication [11]

1.2.2 RF measurements and results of seamless cavities

Cavities after spinning must be internally tumbled or mechanically grinded, then simply chemical polished. Low temperature radiofrequency tests have proofed that the seamless approach and in particular spinning is a solution worthwhile to pursue.

Spun cavities was sent to CERN, DESY, TJNAF and to KEK for characterization. CERN proved that spun copper mono-cells are superior to hydro-formed ones, because of lower losses and lower Q-slope. Accelerating fields up to 25 MV/m was measured at DESY on 1.3 GHz Niobium mono-cell cavity; At KEK and CERNM, the accelerating fields achieved 40MV/m on mono-cell and 25MV/m on 3-cell cavity, a 9-cell has not been tested yet.

1.3 6 GHz cavities

The R.F. characterization of samples is a useful diagnostic tool to accurately investigate local properties of superconducting materials. However the most common limitation of such a system, consists often in the difficulty of scaling the measured results to the real resonator [12].

Using 1.3/1.5 GHz resonant structures cavities is obviously the most direct way, but would be too onerous both for the material cost and the cryogenic expense. Instead, the micro-cavities that completely equal in shape to the real scale model would be the best and most direct way for measuring material R.F. properties.

Using the spinning technique, it becomes feasible to produce small scale resonators in little time, negligible cost and in large quantity.

In INFN-LNL, large number of 6 GHz cavities made of Niobium, Cooper, Lead, even Iron (Figure 1.6) have been produced by spinning technique to study the effectiveness of innovative surface treatments, new thin film deposition techniques, new superconducting materials for RF applications.

Figure 1.6 Picture of 6 GHz cavities made by different material. From left to right are Niobium cavity (thickness 3mm), lighten Niobium cavity (thickness 2mm), Cooper cavity, Iron cavity and Lead cavity.

1.3.1 Advantages of 6 GHz cavities

6 GHz cavities, which geometry shown in Figure 1.7 are made from the remaining material of larger cavities fabrication using spinning technology, they don't need welding (even for flanges) and finally they can be directly measured inside a liquid helium Dewar. With 6 GHz cavities it is possible to perform more than one RF test per day, while 1.3/1.5 GHz cavities need no less than 1 week time preparation for the RF test.

With a tool like this it is possible to study traditional and innovative surface treatments and to perform RF tests on a large amount of cavities with a research budget much lower than the one necessary to treat and tests real cavities. It is also possible to study new thin film superconducting materials grown for example by sputtering or thermal diffusion.

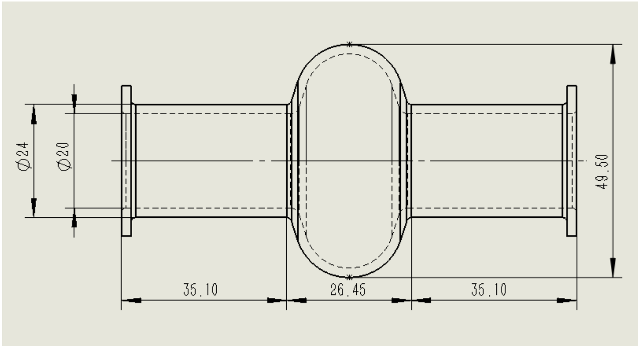

Figure 1.7 The 6 GHz cavity geometry

Summarily, the spinning seamless technology has several advantages in comparison with welding one [13]:

- no welding;
- short fabrication time;
- equipment could be adapted for any size of the cavity, and any quantity of cells;
- comparably low fabrication costs;
- no intermediate annealing;
- almost no scraps;

1.3.2 Drawback

A die (see Figure 1.8(a)) has exactly the same shape of the cavity interior, composed of three collapsible mandrels is used to guide the material when spinning.

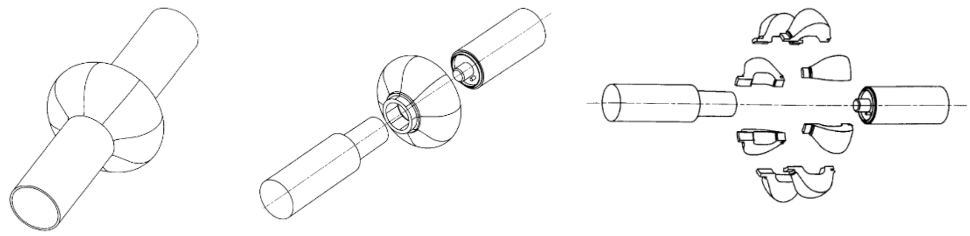

(a) (b) (c)

Figure 1.8 (a)Drawings of the die, which is composed of two cylinders and a shell, assembled and ready for the spinning operation; (b)Disassembled when partially extracted after spinning; (c)Exploded view of the nylon shell of the die with all its ten sectors.[14]

In order to extract the die from the final resonator, two things are taken into account:

1) The central mandrel is Nylon shell, which composed of eight sectors (Figure 1.8(c)), locked together by the two steel cylinders. It is cut symmetrically along a longitudinal plane two four pairs of identical and opposite sectors.
2) Pure motor oil is used as the lubricant between the die and resonator.

Evident vertical scratches (see Figure 1.9) were extruded in the inner surface of the cavity due to the using central mandrel; cavity must be electropolished or chemical polished of the internal surface immediately after spinning, and then immersed in an ultrasonic bath to remove oil contamination.

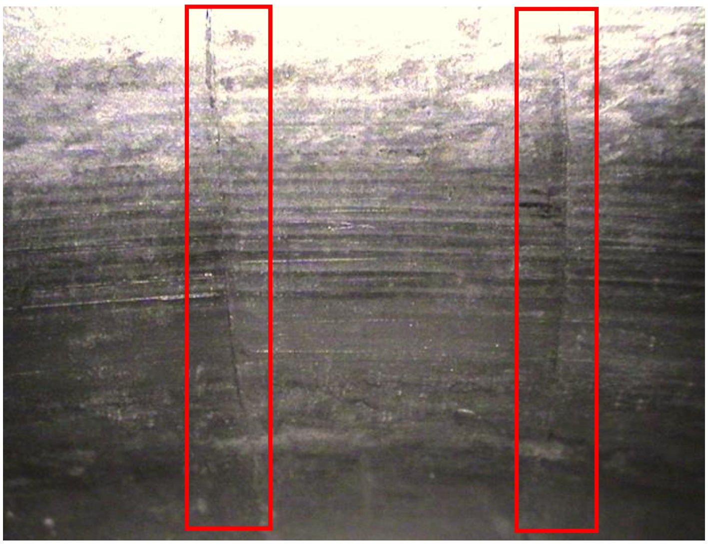

Figure 1.9 Image of inner surface at the center of the cavity, two evident vertical scratches shown in the red rectangles.

1.3.3 Standard surface polishing techniques

The spinning process implies material surface defects, stress and dislocations. The cavity cell is characterized by the presence of evident vertical scratches due to the used mandrel. Obviously the internal surface finishing of a resonant structure is directly correlated to its performance, especially at high fields. Moreover, the lubricant, necessary for the metal mechanical processing can contaminate the used material. The idea is to make the surface smooth and free from contaminants.

There are four techniques used for material removal in 6 GHz cavities: Tumbling, Lapping, Buffered Chemical Polishing (BCP) [15] and Electro-Polishing (EP) [16].

- Tumbling

Tumbling is one of the mechanical polishing treatment, using the abrasive media to remove the defects. Usually it is done by Centrifugal barrel polishing (CBP) machine.

During mechanical treatment, it is necessary to monitor the weight and the morphology of inner surface changing after each tumbling for each cavity.

Mechanical polishing treatment of 6 GHz cavities is the core content of this thesis that will be discussed in detail in later chapters.

- Lapping

After finishing the mechanical polishing of internal surface of cavity, the flanges needs to be lapped flatly using the metallographic polishing machine (Figure 1.10). The aim of this step is to avoid the vacuum leaking during the cryogenic RF test.

At the beginning of lapping, the big roughness abrasive paper would be better for the burrs. Then change to low roughness one, which will increasing the smoothness of the flanges. Finally, using the alcohol as the polishing liquid instead of water. After lapping, it is necessary to make precise washing of cavity in ultrasound bath with soap in few steps and rinsing with acetone and ethanol.

Figure 1.10 Metallographic polishing machine with sandpaper

- BCP

Buffered Chemical Polishing (BCP), in use for over 20 years, is recognized to be the most reliable and stable process. The composition of the mixture is 1:1:2 in volume of hydrofluoric (HF 49%wt), nitric (HNO_3 69.5%wt) and ortho-phosphoric (H_3PO_4 85%wt) acids, with a viscosity, at room temperature, of 0.022 Pa-s and a density of 1545 kg/m^3 [17].

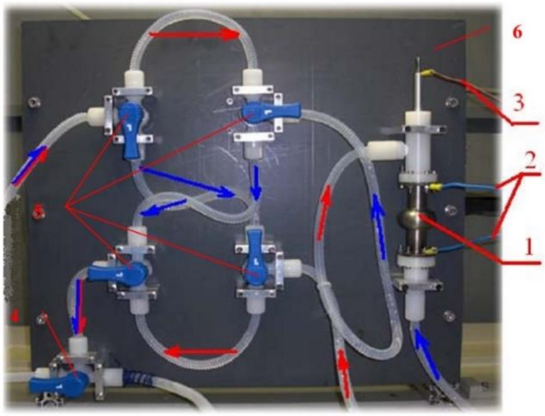

Blue indicator – direct flow, red – indirect.
1 – cavity kit; 2 – anode contacts; 3 – cathode contact; 4 – outgoing valve; 5 – flux regulating valve; 6 – stand.

Figure 1.11 The stand for BCP and EP

As one of chemical treatments, BCP, performed using the standard mixture of acids, removes the possible niobium sub-oxide and contaminants, resulting in a smoother inner surface of the cavity.

In our case, 6 GHz cavity is treated by a small system as the one present in Figure

1.11, which designed for both traditional surface chemical treatments: BCP(does not require cathode) and EP (require cathode) in INFN-LNL.

After the BCP, 300μm thickness corresponding to around 30 grams damage layer is removed.

- EP

Electro-Polishing is believed to be the most desirable treatment for SRF cavities [18], the principle of which is presented in Figure 1.12. EP is an anodic electrochemical treatment carried out in concentrated hydrofluoric-sulfuric (HF-H_2SO_4) acids electrolytes in proportions 1-9.

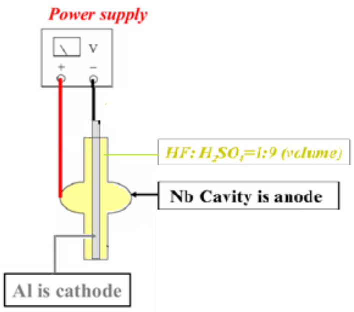

Figure 1.12 The schematic diagram of EP

- HPR

High pressure rinsing (HPR) is nowadays routinely used in the process of superconducting RF cavities assembly to remove residuals from the resonator wall. The pressure of high pure water is about 100 MPa. It is successful in improving cavity performances, mainly reducing field emission. It is usually done before the RF test.

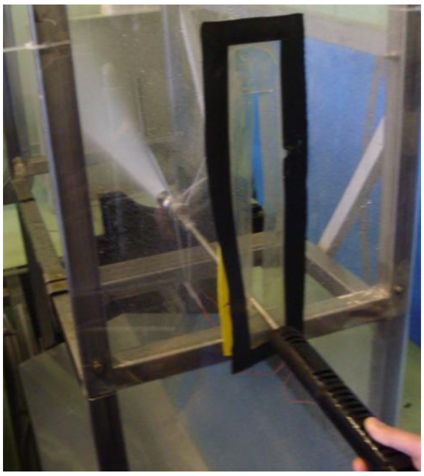

Figure 1.13 HPR for 6 GHz cavities in LNL-INF

Chapter 2

Mechanical polishing approaches

Cavity defects compromise the achievable values of Q-factor and accelerating fields. Mechanical polishing is the first and impartment step to eliminate defects in the cavity interior.

In order to develop a high erosion rate, stable, cheap and safe apparatus, many commercial product like Turbula and some custom designed devices like Zigzag tumbler, CBP and polishing brush have been applied and studied to polish the 6 GHz spun seamless cavities. Some of them run with unsatisfying erosion rate, while other works unstable for long time and it will cost more time and money to repair them when problem happens. But finally, a new mechanical polishing system based on vibrator, with good performance was invented. It will be detailed introduction in the next chapter.

2.1 TURBULA® Shaker-Mixer

Figure 2.1 TURBULA® Shaker-Mixer (model T2F) and 6 GHz cavity

TURBULA® Shaker-Mixer presented in Figure 2.1 is one product from Glen Mills Inc., it is used in many exacting powder blending and mixing applications [19], such as used for homogeneous mixing of powders or different wet components with differing specific weights and particle sizes. But it also includes the application for metal finishing, intricate precision parts can be deburred and polished without damage.

It is composed of plastic container, elastic bands, crowns, and tensioning tool. The mixing container is set into three-dimensional movement that exposes the product to always changing, rhythmically pulsing motion; the exceptional efficiency comes from use of rotation, translation and inversion according to the Schatz geometric theory; the speed change is by the step pulley.

The cavity was filled with the abrasive media and assembled to the plastic cylinder shell with the configuration shown in Figure 2.2. Then the cylinder was mounted to the tumbling container utilizing its unique clamping system. It is available to modify the frequency of tumbling and set the run time.

The characteristics of this tumbler are safe, quiet, but low erosion efficient, 15mg/h is of the maximum value up to now. It could be ascribed to the frequency of the movement, which could not be set at very high, otherwise the system would be very unstable and easily broken.

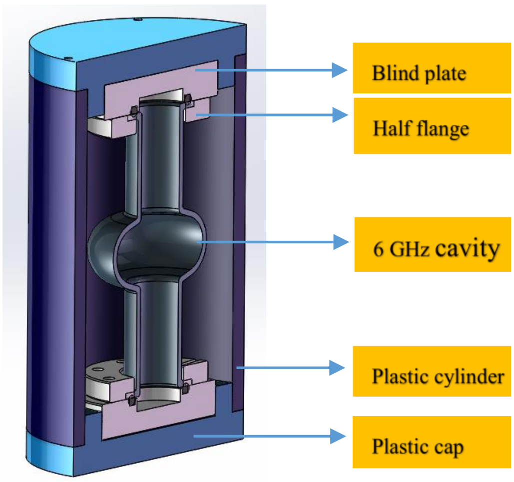

Figure 2.2 The section of the configuration of cavity before mounting to the TURBULA® Shaker-Mixer

2.2 Centrifugal barrel polishing (CBP)

CBP is considered a valuable method that limits the use of harsh chemicals, which would decrease the environmental impact of the surface treatment process while increasing the smoothness of the surface.

The studying of the centrifugal barrel polishing began in the mid to late 1990s. As one of the mechanical polishing equipment, the first CBP system was first build at KEK, High Energy Accelerator Research Organization (KEK) by Kenji Saito & Tamawo Higuchi, and adopted by many other laboratories around the world, the Thomas Jefferson National Accelerator Facility (JLab), the Raja Ramanna Centre for Advanced Technology (RRCAT), Fermi National Accelerator Lab (Fermilab) and so on. A mirror like finishes on the 1.3GHz Tesla-type cavity SRF surface has been produced in Fermilab. All these labs designed their own system or bought industrial machines based on the same principle: mechanically polished the inner surface of the SRF cavities by rotating them at high speeds while filled with abrasive media, which is shown in the Figure 2.3.

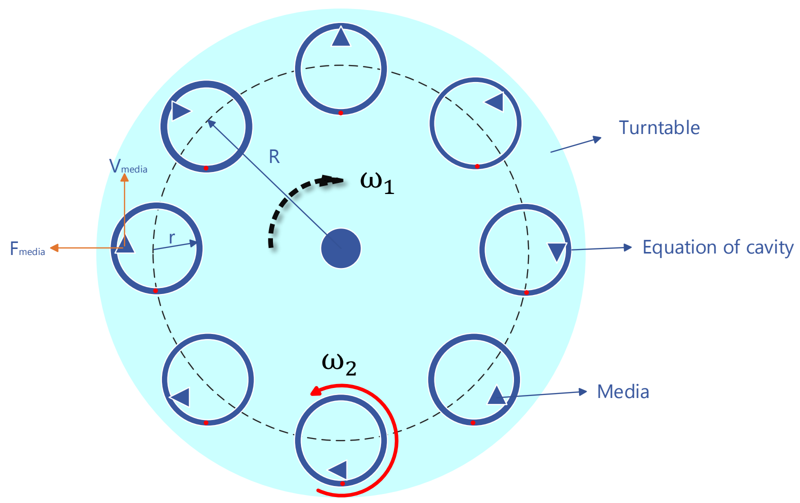

Figure 2.3 Schematic diagram of the Centrifugal barrel polishing (CBP). The red point is the reference point when the angular velocity of the barrel related to the turntable ω_2 equals to zero.

The tangential speed of the media sliding on cavity wall was calculated with the formula

$$V_{media} = (\omega_1 + \omega_2) \times r \tag{2.1}$$

Where,

- ω_1 - Angular velocity of turntable;
- ω_2 - Angular velocity of cavity related to the turntable;
- r - Radius of the cavity.

The centrifugal force of the media is

$$F_{media} = \frac{mV_{media}^2}{R+r} \tag{2.2}$$

Where，

- m - Mass of the media;
- R - Radius of the trajectory of cavity.

In INFN-LNL, one CBP system presented in Figure 2.4(a) was developed several years ago, in which the $\omega_2 = 0$, worked properly and with high erosion rate. The dimension was not so big that it save much lab space. In this system, six 6 GHz cavities were tumbled together by fixing them in two groups like the way shown in Figure 2.4(b).

But in the CBP process the whole system was shaken due to only one barrel spin around a central shaft. In this situation, the central shaft endured a big tensile force when work at high revolving speed and would be broken after a long time working.

At present, the CBP machine has been industrialized (Figure 2.5), which used for 9 cells TESLA-type cavities tumbling. There are two or four barrels at axial symmetry position. Each barrel spins around its own axis at the same speed and in the opposite direction as the main shaft. This secondary rotation of the barrel around its own axis greatly reduces processing time (Figure 2.6).

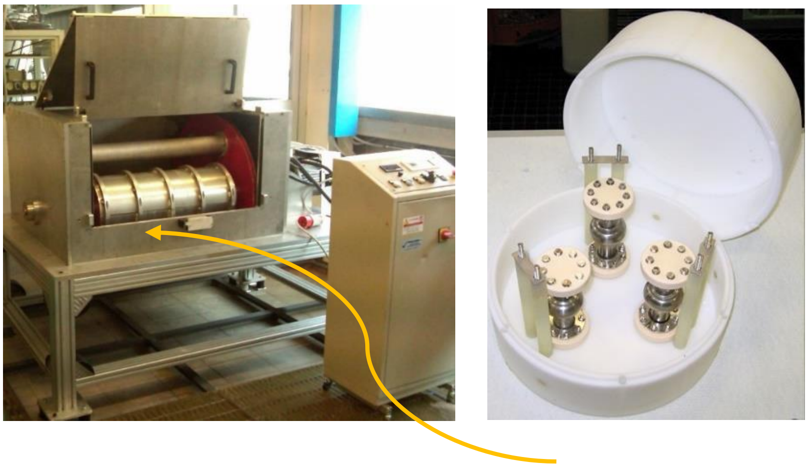

(a) (b)

Figure 2.4 (a) Photograph of the CBP system in INFN-LNL. (b) The configuration of the cavities.

Figure 2.5 Industrial centrifugal barrel polishing machine

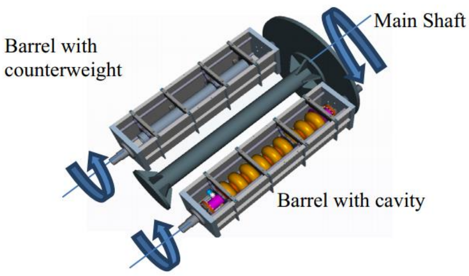

Figure 2.6: Schematic of main shaft and 2 barrels of a centrifugal barrel polishing machine denoting the directions of rotation. This is a model of the Fermilab machine with a 9-cell Tesla – type cavity and counterweight shown in the barrels [20].

2.3 Zigzag tumbler

The tumbler presented in Figure 2.7, which named zigzag tumbler, was another attempting to polish the cavity in an easy, cheap way. The cavity was filled with abrasive media and blocked off by two plastic plugs in both terminals, then put into the tumbler and sealed by the cap (Figure 2.7 (c)). When the tumbler turned by pivoting its center shaft with a high speed, the cavity was rotated by the zigzag style. The media in the cavity was not rotated so fast as the cavity due to the force of gravity itself, therefore a relative movement is exit between the cavity and the media.

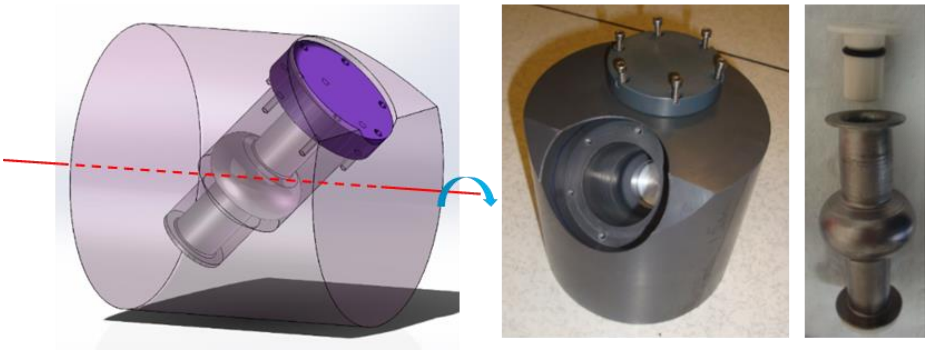

(a) (b) (c)

Figure 2.7 The 3D drawing (a) and entity (b) of the zigzag tumbler

Two different way which called dry polishing without water and wet polishing with water were tested, but there is no essential difference between the two results. In both situation, the erosion rate of zigzag tumbler was not as high as expected due to the small force inflicting to the inner surface of the cavity, although with a very high turning speed.

2.4 “Flower brush”

2.4.1 “Flower brush” design for polishing 6 GHz cavities

Polishing brush is one product that mainly used for deburring, fine grinding and other processing for the parabolic surface. It is mainly composed of the iron wire as a skeleton, with lots of neat rows of fine brush filaments stretching outwards (Figure 2.8). The material of brush wire is nylon yarn, fiber hair, bristle, steel wire, copper wire, abrasive wire and so on, have different scope respectively.

The polishing brush on the market was usually used to polish the inner surface of tube, whose diameter equal everywhere. For 6 GHz cavities, the dimension of two terminals are small and the center is bigger, while the center is the aim region should be mainly polished, therefore, the brush mentioned above is not suitable obviously.

So it needs to design a customized brush that can go to the center of the cavity and can change the angle in order to polish the whole area inside. Base on this idea, a brush was machined and assembled, whose 3D drawings was shown in Figure 2.9. As its special shape of the head and angle changeable leafs look like one flower, we call it “flower brush”. The whole “flower” is made in stainless steel (Figure 2.10), and the holes in the “leaves” was used to fix the abrasive material (shown in Figure 2.11), which is suggested to be wear-resistant material.

Figure 2.8 Polishing brush on the market

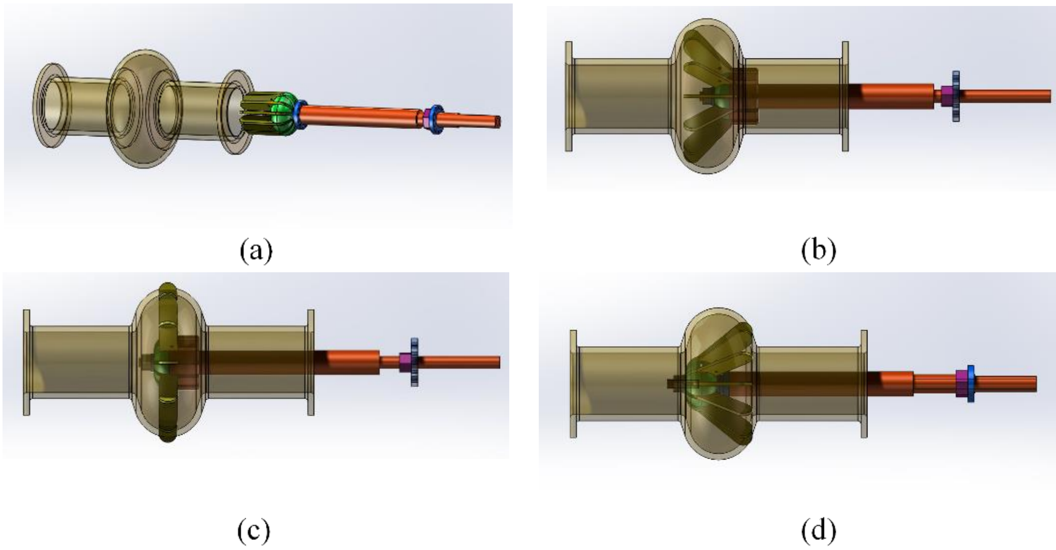

Figure 2.9 3D drawings of “flower brush”.

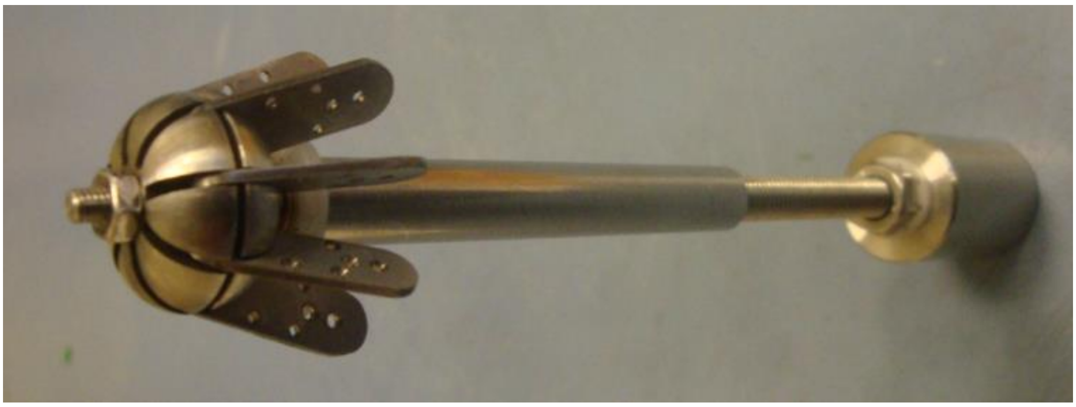

Figure 2.10 Photograph of “flower brush”.

(a) (b)

Figure 2.11 Abrasive material. (a) Sand paper; (b) Scotch Brite

Before putting the “flower brush” into the cavity, the abrasive material were fixed to the leaves of the “flower”, which presented in the Figure 2.12. We can test different abrasive material just by changing the “leaves” conveniently.

(a) (b) (c)

Figure 2.12 “flower brush” with abrasive material.

When the leaves are ready, the petals are drawn in together as shown in the Figure 2.9(a) and pushed into the cavity, which is fixed on workbench well, then the brush is rotated by the driving of a handing , due to the centrifugal effect, the blades open automatically Figure 2.9 (b, c). Its angle can be changed by a thin line pulling wire by adjusting the position of the nut (Figure 2.9(d), the line is not shown). Thus it ensures each place of the interior surface of the cavity can be brushed, i.e., the inner surface of the center part of the cavity can be polished back and forth.

2.4.2 Polishing test

- Test on lathe with abrasive paper
  a) The cavity was clean in the ultrasonic bath, flushed with the ethanol and dried with nitrogen before polishing;
  b) Fixed the cavity on one terminal of the lathe, which can move back and forth;
  c) Fixed the “flower brush” on the other terminal of the lathe, which can rotate;
  d) Put the “flower brush” into the cavity like Figure 2.13, then run the lathe, which

rotation speed was 750 rpm, shown in the Figure 2.14.

Figure 2.13 The way of putting "flower brush" into the cavity.

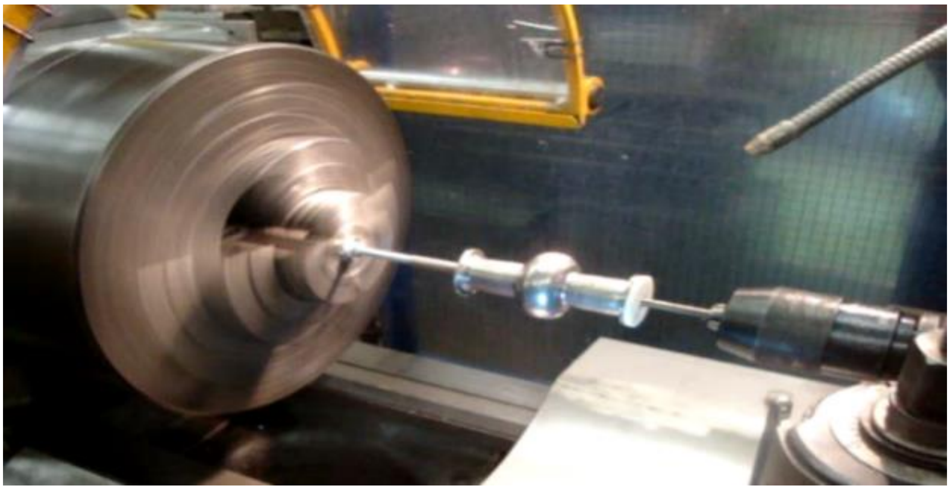

Figure 2.14 The "flower brush" was polishing the cavity on the lathe.

- Polishing test driven by the pneumatic hand held polisher.

The pneumatic hand held polisher was driven by air and its rotating speed was much higher than the lathe.

a) Mounted the "flower brush" to the pneumatic hand held polisher (Figure 2.15).
b) Fix the cavity on the workbench.
c) Put the "flower brush" into the cavity and launch the pneumatic hand held polisher (Figure 2.16).

Figure 2.15 The petals were spreading in high rotating speed

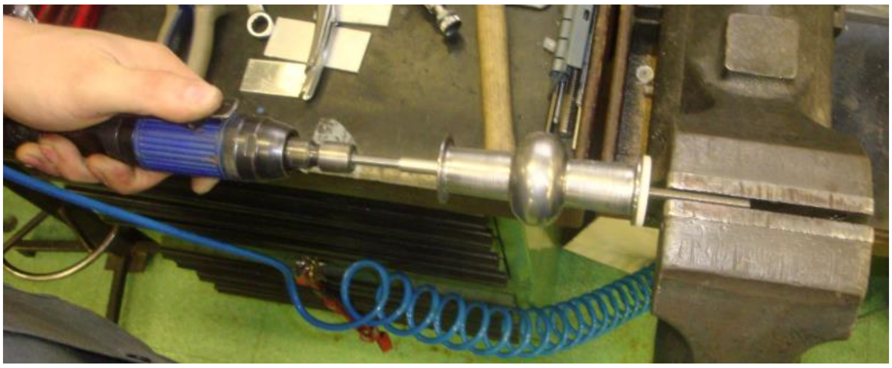

Figure 2.16 Polish the inner surface of cavity by pneumatic hand held polisher using "flower brush".

- summary of "flower brush" tests
  - (i) In the lathe test, the polishing effect was not good due to the low rotating speed.
  - (ii) But with a higher speed in the test 2, the sand paper was nearly broken in a short time with the high rotating speed and should be changed frequently.
  - (iii) Scotch Brite in Figure 2.12 (c) is thick, so it is permitted to mount only 4 pieces, otherwise, the head of brush can't be put into the cavity.
  - (iv) In a short time, the Scotch Brite was also nearly broken.
  - (v) 0.134g internal material of cavity removed in 2 minutes, which seems promising.

Chapter 3

Vibrating system - a new mechanical polishing approach

After a long time exploration, a vibrating system was realized and studied to improve the erosion rate for different material cavities. This chapter will focus on how this system was developed step by step.

3.1 Industrial application of vibrator

A vibrator is a mechanical device to generate vibrations by an electric motor with an unbalanced mass on its driveshaft.

Vibrators are used in many different industrial applications both as components and as individual pieces of equipment [21].

Vibratory feeders and vibrating hoppers are used widely in the pharmaceutical, food, and chemical industries to move and position bulk material or small component parts. The application of vibration working with the force of gravity can often move materials through a process more effectively than other methods. Vibrating screens are used to separate bulk materials in a mixture of different sized particles. Vibrating compactors are used for soil compaction especially in foundations for roads, railways, and buildings. Concrete vibrators consolidate freshly poured concrete so that trapped air and excess water are released and the concrete settles firmly in place in the formwork.

3.2 Resonance-the original idea

Resonance phenomenon is refers to the mechanical system by excitation frequency and the system of a certain natural frequency were close, system amplitude increase significantly. And this excitation frequency is called resonance frequency. The input energy of motivate to the mechanical system is the largest when resonance. A system of many objects can have more than one resonance frequency.

According to this idea, we design a combined spring vibration system, which configuration is shown in Figure 3.1. The square object with the mass m is the vibration source, which makes the upper and lower two springs vibrate in the landscape orientation in small range. Both springs have same stiffness k_0, the original length is l_0. At the equilibrium position, they are elongated to l_1 and l_2, both sides of the object under tension T_1 and T_2. Now the object in the lateral direction (the x direction) for a slight vibration, then the equivalent stiffness of this combination spring of the vibration system and the system natural frequency can be derived as follows.

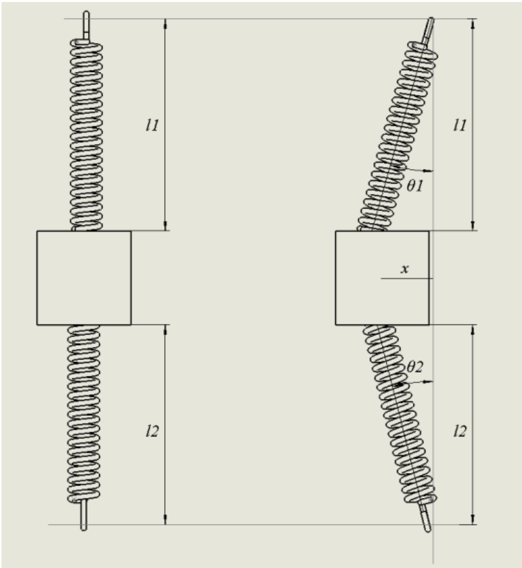

Figure 3.1 The configuration of combined spring vibration system

Objects in the x direction by the (0, 0) moves to the (x, 0) position, the upper and lower spring extension individually from l_1 to $\sqrt{l_1^2 + x^2}$ and from l_2 to $\sqrt{l_2^2 + x^2}$, then the size of the spring restoring force is

$$T_1 = k_0(\sqrt{l_1^2 + x^2} - l_0) \quad (3.1)$$

$$T_2 = k_0(\sqrt{l_2^2 + x^2} - l_0) \quad (3.2)$$

The force to the objects includes both sides of the spring tension and the gravity, the total force is zero, so no motion in the y direction. Two component of spring tension T along the x-direction are

$$\mathrm{F} = T_1 sin\theta_1 + T_2 sin\theta_2 \quad (3.3)$$

Where,

$$T_1 = -k_0(\sqrt{l_1^2 + x^2} - l_0) \quad (3.5)$$

$$T_2 = -k_0(\sqrt{l_2^2 + x^2} - l_0) \quad (3.6)$$

$$sin\theta_1 = \frac{x}{\sqrt{l_1^2 + x^2}} \quad (3.7)$$

$$sin\theta_2 = \frac{x}{\sqrt{l_2^2 + x^2}} \quad (3.8)$$

This force causes the object accelerate along the x direction to return to the equilibrium position, so it is

$$\mathrm{F} = T_1 sin\theta_1 + T_2 sin\theta_2 = -k_0\left(1-\frac{l_0}{\sqrt{l_1^2+x^2}}\right)x - k_0\left(1-\frac{l_0}{\sqrt{l_2^2+x^2}}\right)x \quad (3.9)$$

$$F = -k_0\left(2-\frac{l_0}{\sqrt{l_1^2+x^2}}-\frac{l_0}{\sqrt{l_2^2+x^2}}\right)x = m\frac{d_x^2}{dt^2} \quad (3.10)$$

This is the system dynamic equations of vibration. In the x and l take the same order of magnitude of value, this is a second-order nonlinear differential equation. This equation can be seen that the lateral vibration spring oscillator does not belong to simple harmonic motion, but when the object vibrate in small laterally, that **x** << l so $\sqrt{l_1^2+x^2} \approx l_1, and \sqrt{l_2^2+x^2} \approx l_2$ established, the force F acting on the object is proportional to the displacement x of the object, namely

$$F = -k_0\left(2-\frac{l_0}{l_1}-\frac{l_0}{l_2}\right)x = -kx \quad (3.11)$$

Where,

x is the displacement in laterally; k is the equivalent stiffness of the system, equal to $k_0\left(2-\frac{l_0}{l_1}-\frac{l_0}{l_2}\right)$. Vibration dynamic equations are as

$$\frac{d_x^2}{dt^2}+\frac{k}{m}x = 0 \quad (3.12)$$

This is the dynamic equations of simple harmonic motion. This equation can be obtained natural circular frequency of the system

$$\omega_0 = \sqrt{\frac{k}{m}} = \sqrt{\frac{k_0}{m}\left(2-\frac{l_0}{l_1}-\frac{l_0}{l_2}\right)} \quad (3.13)$$

And the system natural frequency is

$$\nu_0 = \frac{1}{2\pi}\sqrt{\frac{k_0}{m}\left(2-\frac{l_0}{l_1}-\frac{l_0}{l_2}\right)} \quad (3.14)$$

The natural frequency not only relies on the system oscillator mass m, the spring parameters l_0, k_0, but also on the initial state of the system l.

3.3 Experiment with small vibrator

3.3.1 The first experiment

There is no information reported till date in tumbling process using vibrator technique for cavities in SRF field. Transferring the idea into reality often takes some time and it will not know the eventual result until a large number of tests been done.

Firstly, an idle vibrator with small dimension and power of 22 Watts was tested (Figure 3.2). The components of the system were assembled in a very easy way.

The vibrator and the cavity are hung by two springs and a piece of plastic plate, shown in Figure 3.3. The springs connected with two adjustable rod. The cavity is closed by two blind flange and fixed by Aluminum plates, which composed by two halves. Two pieces of 1 mm thick rubble with grease were clamped between the cavity and the Aluminum plates, playing a role in cushioning and lubrication. The polish material, such as silicon carbide, silicon oxide and water, were put inside the cavity. The whole stuffs before assembled are shown in Figure 3.4.

Figure 3.2 Picture of the firstly using vibrator

Figure 3.3 One example of the vibrator system for 6 GHz cavity

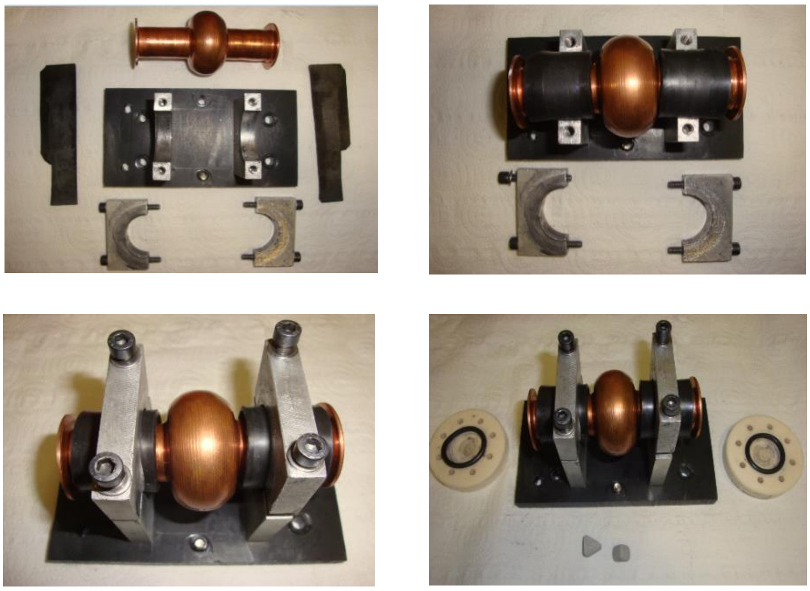

Figure 3.4 The diagrams of Assembly process before hanging up

The vibrator works at single phase Alternating Current (AC) 220 Volts with Power-Frequency (50Hz). After switch on, the cavity was vibrated with the springs, and the sound of media polishing the surface was clear, what’s more, the cavity can turn spontaneously when vibration, while the black rubber was not move as its elasticity and effect of the grease.

There are some advantages of this system:

1) The structure is simple, and it is easy to assemble and disassemble all the parts;

2) Tightness of the spring is adjustable, means the intrinsic frequency in landscape orientation can be changed equally to the vibrating frequency;

3) It can rotate itself that makes available to tumbling uniformly to the inner surface without bearings and motor driving.

On the other hand, this system also has some disadvantages obviously:

1) The grease add between the rubber and the cavity contaminates the external surface of the cavity, hence need to clean more often;

2) Sometimes the cavity stop rotate due to the blocking with the sheet rubber, it may cause inhomogeneous removal of inner material;

3) The rotation direction of the cavity can't be control without other auxiliary equipment;

4) The vibration frequency is not changeable.

3.3.2 The second experiment

In order to eliminate the negative factors, and sometimes we don't want to clean the cavity after tumbling, for example, tumbling spotless cavity with Tin. Therefore the targeted improvements should be conceived. We tried to use two bearings instead of Aluminum plates to connect the two flanges of cavity to avoid the contamination to the outer surface of the cavity,

Firstly, the ordinary bearings fixed by two U-clamps are used shown in Figure 3.5, but the cavity can't rotate itself well unless the bearing center, connection axis center, cover center and cavity direction center are in alignment, in which situation rotate with a smaller mechanical stress.

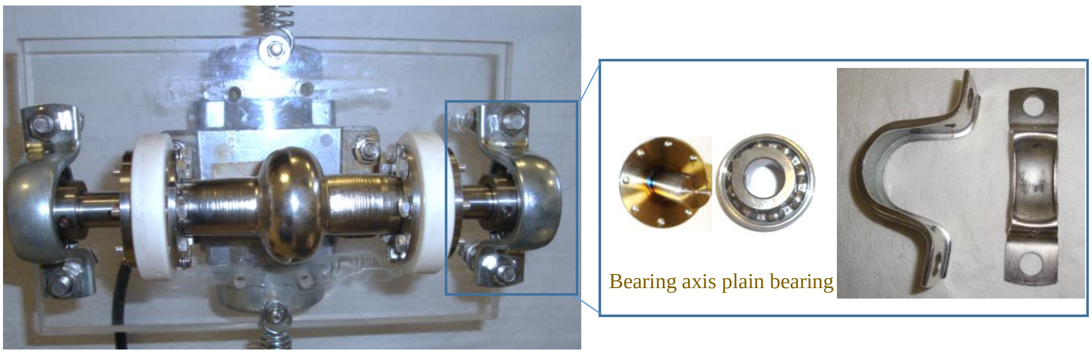

Figure 3.5 A complete mechanical (Vibrator) process-cavity mounted on vibrator through PMMA-glass (15 mm thick) support plate (transparent in figure)

To solve this problem, self-aligning bearing was recommended and new bearing holders were designed and fabricated (see Figure 3.6).

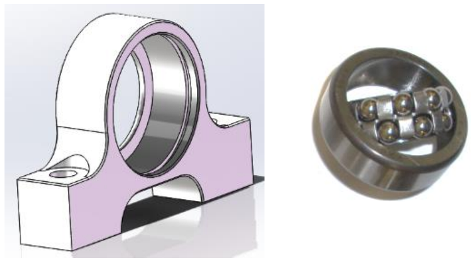

Figure 3.6 Drawing of bearing holder and image of self-aligning bearing

After this, the mechanical configuration of the cavity was basically solved and the new setup is shown in Figure 3.7, in which the cavity is sealed with half flange, O-ring, plastic blind flange and drive axis by M5 hex bolts; the self-aligning bearing is fixed into the bearing holder tightly and locked on the drive axis by the snap ring; the belt axis (shown detailed in Figure 3.8,) is connected to the drive axis.

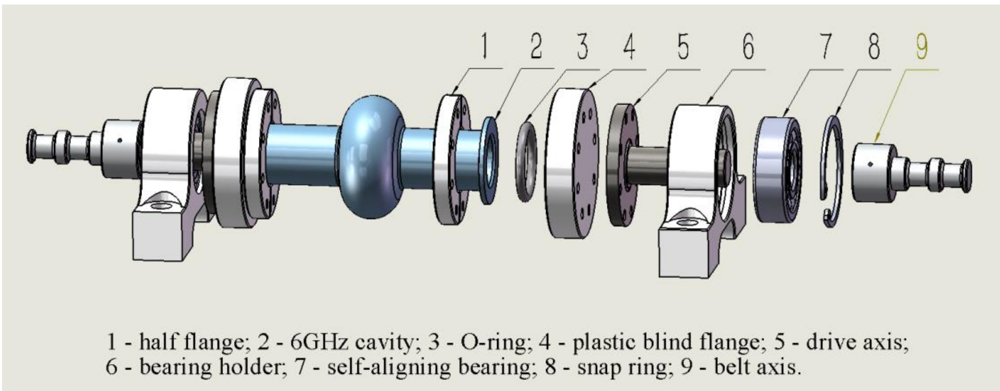

Figure 3.7 Drawing of mechanical configuration of the cavity. The assembled state is at left, and the Exploded Views is at right.

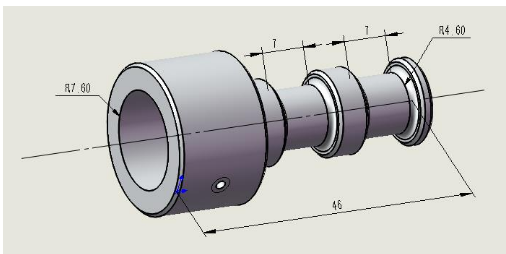

Figure 3.8 Drawing of the belt axis

3.4 Vibrator system for 6 GHz cavities

After determined of the mechanical configuration of the cavity, adjustable frequency vibration source, brackets, resonant spring, plate, drive motor, drive belt also requires careful design and carefully selected.

3.4.1 Vibrator

Figure 3.9 is the internal structures images of one commercial foot mounted electric vibrator which was chosen in the system. The type is MVSI 15/35 – S02, with centrifugal force 30.2kg, weight 5.6kg, max input power 85W, max current 0.21A at 50Hz. Power supply in our case is three-phase voltage ~400V.

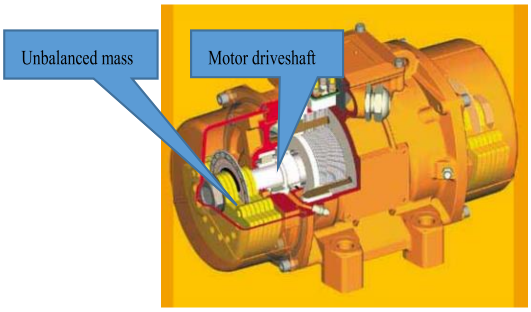

Figure 3.9 The internal structures images of one commercial vibrator

Due to the strong and fast vibration during the polishing processor, everything refers to the vibrator should be designed specially. For example, the power supply cable at the connection box should be isolated by sponge, otherwise the cable may be broken-down (see Figure 3.10) after a long time impact to the box or some harder place.

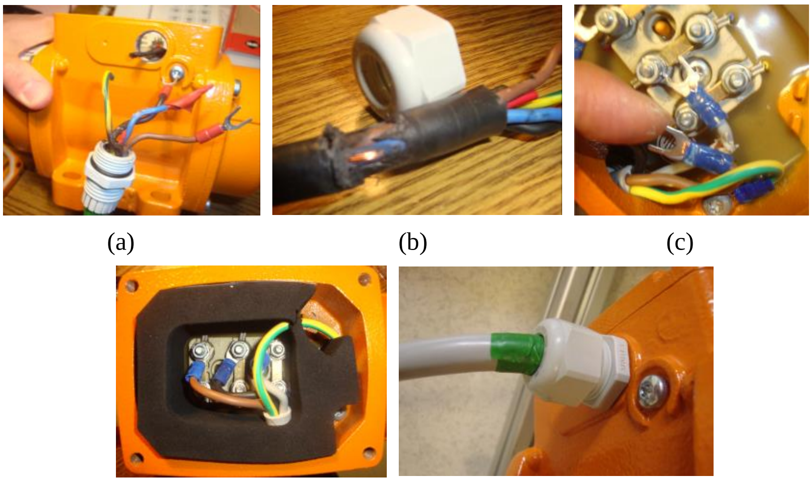

(a) (b) (c)

(d) (e)

Figure 3.10 Images in first line is the consequence after neglecting the sponge, while in second line is the wright connecting way. (a) The cable was broken-down; (b) the cable was hurt by the shroud; (c) the cable was hurt by the cable jointing sleeve; (d) using the sponge to save the cable; (e) using electrical adhesive tape to protect the cable.

3.4.2 control box

The main role of the control box is to provide a three-phase adjustable frequency power to vibrators, and power supply to the rotating motor and cooling fan. In the front panel, it allows to start, stop, and change the frequency etc., the rear panel is a power supply input and output interfaces.

Only the Variable-frequency drive (VFD) and filter are arranged in the chassis, so space for heat dissipation is much enough.

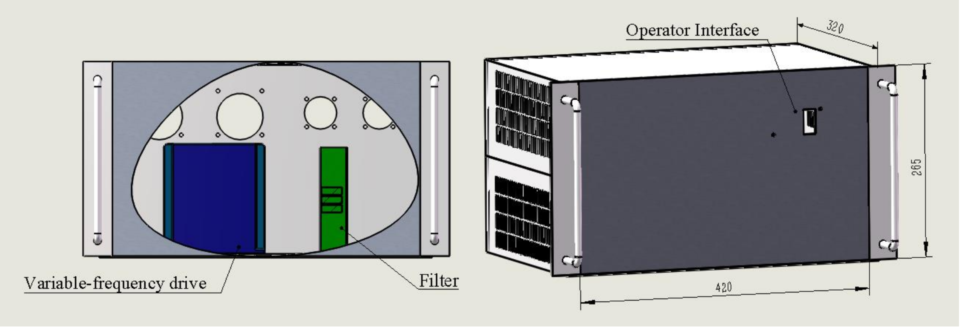

Figure 3.11 Sectional view of the inner and chassis dimensions

Figure 3.12 is one part of the internal electrical wiring diagram.

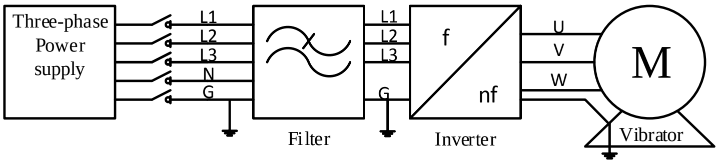

Figure 3.12 Diagram of the electrical connection

- **VFD**

As described in the 3.1, commercial vibrators work at fixed frequency, mostly at 50Hz, our vibrator is work at or close to the system resonant frequency, which depend on the springs, the mass of the load and the material and the thickness of the plate.

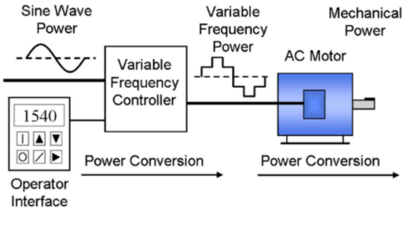

Figure 3.13 The main principle diagram of the VFD [22]

A VFD (also termed adjustable frequency drive, variable speed drive, AC drive, micro drive or inverter drive) is a type of adjustable-speed drive used in electro-mechanical drive systems to control AC motor speed and torque by varying motor input frequency and voltage[23]

Frequency converter (Figure 3.13) is mainly composed of rectifier (ac to dc), inverter (dc to ac), brake unit, drive unit, detection unit, micro processing unit, and drive operator interface. In addition, the inverter contains many protective functions, such as over-current, over-voltage protection, overload protection, etc.

In the vibrator system, we choose the product from Fuji Electric Co., Ltd, the inverter type is FRN4.0E1S-4E (Figure 3.14), which is a standard type without EMC filter built-in. The maximum frequency it can supply is 400Hz.

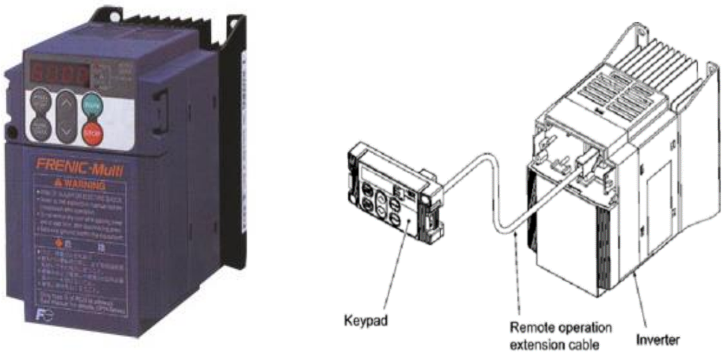

Figure 3.14 Picture of real products FRN4.0E1S-4E which keypad can install to the front panel of the control unit of the vibrating system by the cable with RJ-45 connectors

- **Inverter input filter**

Inverter input filter shown in Figure 3.15 is one kind of the special inverter filter, whose mainly function includes the following aspects:

Figure 3.15 3 phase RFI Filter

a) Inhibition of high order harmonic frequency of converter

The process of rectifying of frequency converter is the equivalent of a high speed switch, therefore, it will produce large amounts of high order harmonic. These higher harmonics, with the flow of power, are brought into the grid, which led to sensitive equipment using the same grid interference;

b) Preventing frequency converter from interference

Frequency converter is an interference source, is also an interfered source, or also called sensitive equipment. If harmonic in the power grid is too high, and harmonic content is too large, the inverter will sent over voltage, over current, overload and other false alarm;

c) Improving system power factor

Inverter input filter, with certain compensation function, can improve the power factor of the whole control system. It also has a certain energy-saving effect;

d) Ease the three-phase imbalance

If the input of the inverter phase imbalance, in the severe cases, it will cause the inverter out of work. Coupled with the inverter input filter, it can alleviate this problem effectively.

3.4.3 Mechanical configuration

As reported in Figure 3.16, the brackets was made of 6 Aluminum profiles, which high is adjustable. The rubber shock absorbers at the bottom are necessary. The plate machined by stainless steel or non-metallic material was hung between the upper and lower two Aluminum profiles by 3 springs using custom nuts (Figure 3.17). The plate in the drawing is suitable for 2 cavities tumbling simultaneously.

The upper two springs fixed by two screws reduce the force of themselves to half assure that they can work for long time without breaking. The bottom spring makes sure the vibrator and cavities stable and the plane of the plate is perpendicular to the horizontal plane. The vibrator is fixed to the plate in the direction that makes the driveshaft perpendicular to horizontal plane. In this situation, the unbalance mass in the vibrator rotate paralleling to the horizontal plane, and don't have to overcome the gravity to do work, so as to improve the conversion efficiency of electrical energy.

In order to polishing the cavity homogeneously, the cavity must be rotated while vibrating. Both the cavities can connect to the motor axis direct of connect in series. Obviously, rigid belt with no elasticity can’t be used here, it must choose one belt with prefect elasticity and long fatigue life.

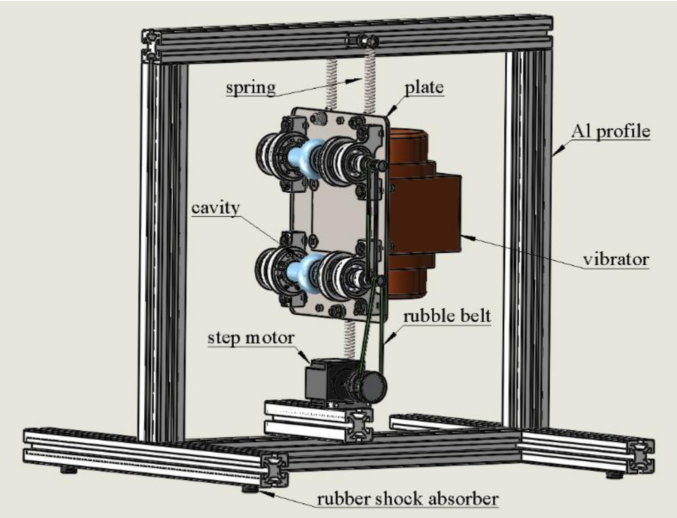

Figure 3.16 Schematic drawing of the vibrating system equipped with two 6 GHz cavities

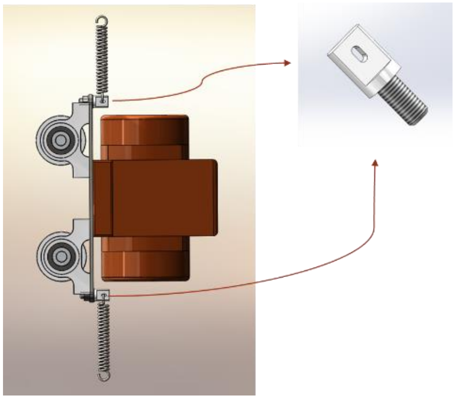

Figure 3.17 connection of the spring and the plate using the custom nuts

The stepper motor (Figure 3.18) mounted at the bottom, contains a control board itself and it is easy to program the motion, for example let the cavity rotate back and forth, fast or slowly, and create the opportunity to find out the effect of the cavity rotation behavior. The motor position also need to be adjustable to suit different length rubble belt. The motor belt wheel (see Figure 3.19) connected to the motor can drive two cavities simultaneously.

Figure 3.18 Image of programmable stepper motor

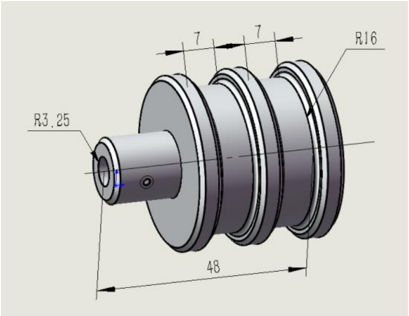

Figure 3.19 Drawing of motor belt wheel

3.4.4 Falling detecting switch

The vibrator is very powerful especially work at high frequency. The springs as one part of the resonance system has the limited fatigue life. It is uncertain when it will break, the direct result of which is the cavity and vibrator fall down to the fall without giving signal to the control system. So spring broken is one potential threaten that may induce the cavities falling down while the vibrator is still working. Such situation happened during the polishing process before. It is certainly need an effective mechanism to detect the falling action and stop the system running, otherwise it may cause secondary damage.

There are two proposed scheme in our case. The first one is piezo-electric accelerometer, which principle diagram is shown in Figure 3.20. It measures proper acceleration (rate of change of velocity), which is the acceleration it experiences relative to freefall and is the acceleration felt by people and objects.

The acceleration of the cavities bound with the accelerometer will change at the moment when they fall to the floor. But measure this acceleration is not the ultimate aim, it need to transfer this value to a digital level (0V or 24V) which as the input to the control system, and it is different to do this without special conversion circuit, which will increase the complexity of system and also may cost much money.

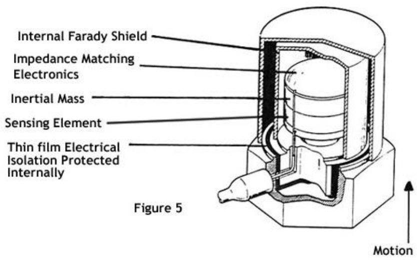

Figure 3.20 The cross section view of the accelerometer [24].

The idea of second scheme comes from the impact sensor which is usually used in the car as the switch of the air bag. The principle is easily understand, and the structure is not complicated (Figure 3.21).

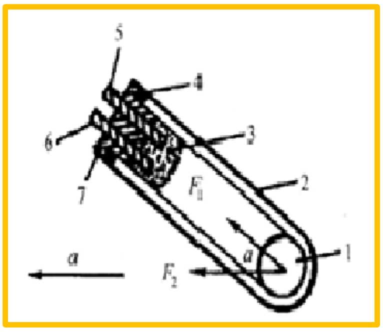

1-Mercury (static position); 2-Housing; 3-Mercury (dynamic position); 4-Ring; 5-Electrodes (contacts firearms); 6-Electrode (connected to power); 7-Sealing plug; α- deceleration; F1-mercury movement direction component; F2-level component; a- the angle between mercury movement direction and the horizontal direction

Figure 3.21 The schematic diagram of impact sensor.

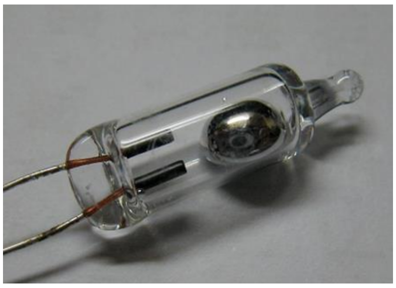

Figure 3.22 One example of the commercial impact sensor.

The commercial one shown in Figure 3.22 may not suitable for our system as the glass housing and the short length. However, it is possible to design a desirable one with any dimension and use similar conductive liquid inside instead of mercury, which may harmful to the environment.

In the design (Figure 3.23), the RF connector was used as the electrodes and sealing plug that simplifies the structure and gets a well sealing. The housing is made by transparent plastic and is easy to machining.

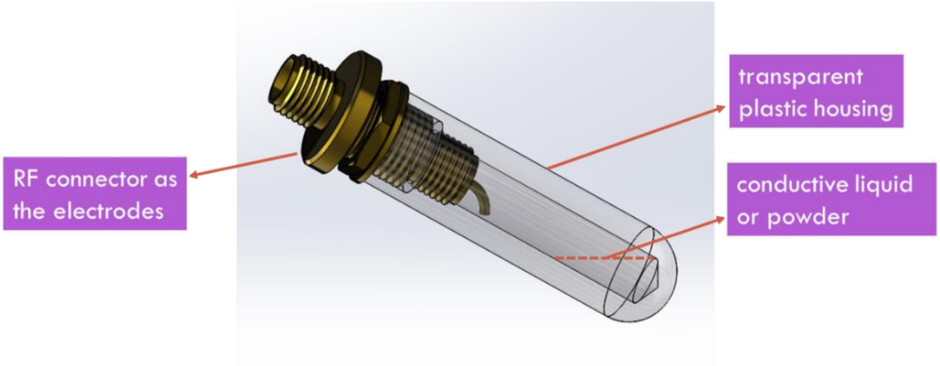

Figure 3.23 The drawing of the custom impact sensor

When falling down happen, the conductive liquid in the housing will short the RF connector and it is easy to transfer this switch signal to the inventor using the circuit presented in Figure 3.24.

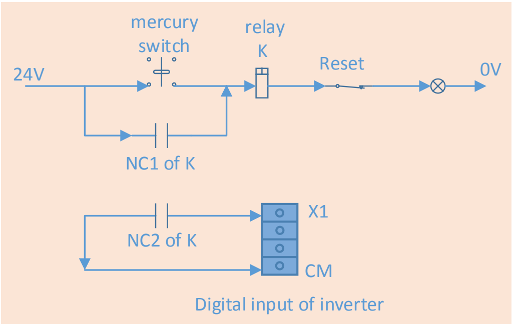

Figure 3.24 Schematic of the trigger capture and fault display circuit.

Components in this circuit include 1 relay with 2 normal open contacts, 1 reset switch (spring switch) and 1 lamp (led 24V) only. And it is easy to connect to the interface of the inventor (Figure 3.25) and determines the work state by setting the corresponding command.

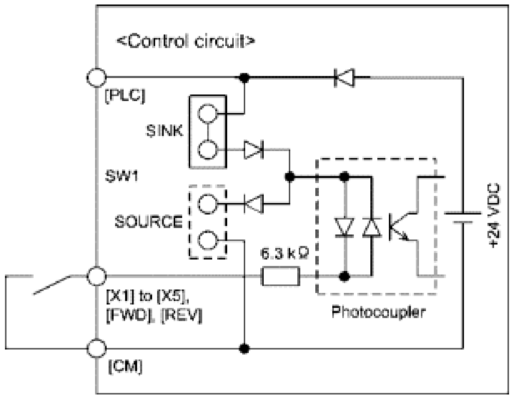

Figure 3.25 The connector circuit in the inventor.

Chapter 4

Automation of the optical inspection system for 6 GHz cavities

Consecutive inspections of cavities in different stages of the surface preparation process allow a monitoring of the evolution of surface defects. It will also be very helpful to put the suitable media inside the cavities during mechanical polishing and establish the right treatment duration to perform the best internal surface finishing if we know the morphology after each treatment. In INFN-LNL, every cavities were taken a record of the inner surface after each mechanical or chemical treatment with the help of an optical inspection equipment.

Generally speaking, every cavity may be tumbled 10 times at least, and taken 20~30 images of inner surface each time. For 100 cavities, 20~30 thousands of images should be token. No only taking picture is a time consuming process but manager and inquire all these pictures is also a heavy job.

In order to improve the efficiency of taking pictures and create a database of images of every cavity after each treatment, the existing optical inspection equipment need to update, including mechanical system upgrades and photo software development.

4.1 Before updating

4.1.1 System introduction

The idea of the optical inspection system is to check an eventual defect evolution before and after each polishing treatment without any risk to touch the internal surface of the small cavity. The system was fabricated a few years ago. It is made up of three parts: miniature camera, mechanical support and one computer. (Shown in Figure 4.1)

It was an artful though to use an intraoral camera to investigate the inner surface of small cavity because the camera was a mature products and the dimension of the camera extremely suitable for the 6 GHz cavity, i.e., the length of the camera head is 94mm, which approximately equals to the length of the cavity; the diameter of the camera head is 12mm, which less than the inner diameter of the cavity, therefore, the camera allows one to take photo anywhere inside the cavity.

The camera and the cavity both can move forward and backward along the guide, in which a graduation ruler measuring the moving distance is attracted by magnets. In addition, the camera can move up and down by modifying the nut. The cavity was put on four small wheels which permit the cavity rotate smoothly. The rotation angle can be measured by the rotundity goniometer.

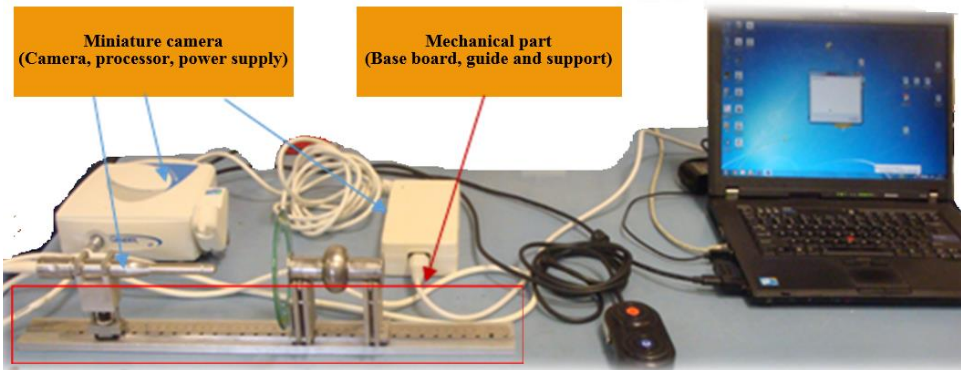

Figure 4.1 The optical inspection equipment before updating

The camera is control by a computer through the Firewire (IEEE 1394A) interface, which can deliver high-resolution digital video for great image quality to the computer. The images are captured by the software offered by the company, which shown in Figure 4.2.

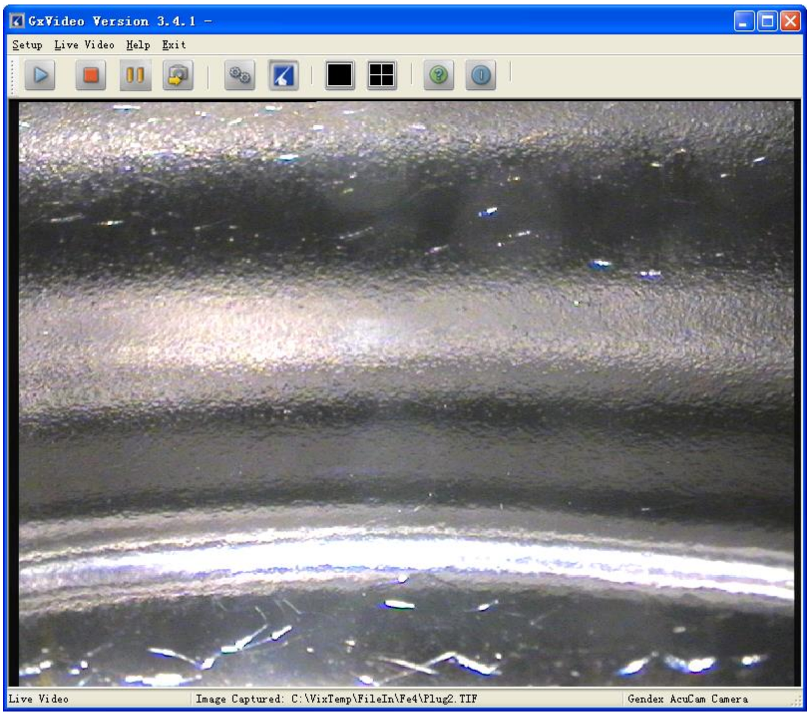

Figure 4.2 Photo software interface

4.1.2 The necessity of the automation

Before updating, the photography process is operated by manual. The cavity can be divided into 5 sections from left to right as reported in Figure 4.3, the left neck, left iris, equator, right iris and right neck. For each section, images should be taken at every 60 degree during the cavity rotating. From left to right, the camera should zoom in or zoom out accurately to focus 5 times due to the cavity shape changing.

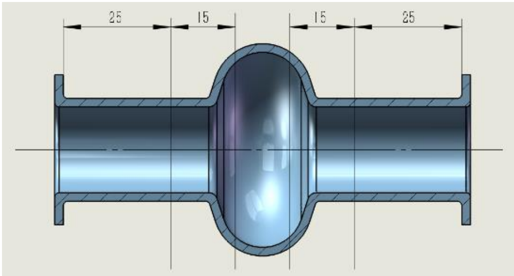

Figure 4.3 The cross section of the 6 GHz cavity

What's more, every image captured by the software have to be rename by hand one by one in order to record relevant information, such as material, weight, tumbling numerical order, date, position and angle.

4.2 The realization of automation

4.2.1 Updating of mechanical part

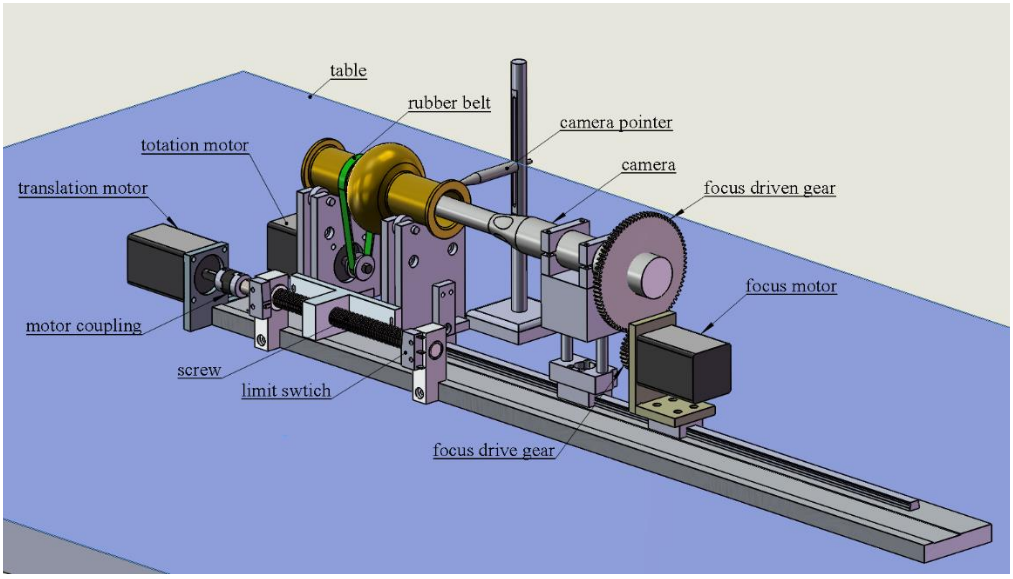

Figure 4.4 3D schematic diagram of the optical inspection system mechanical upgrades

In order to realize automation, 3 stepper motors and relevant auxiliary machineries are added (Figure 4.4). The camera and focus motor are fixed in the rail. The ratio of the focus drive gear and the driven gear is 28:80, which ensure the focusing accuracy. The translation motor rotating the screw by motor coupling moves the cavity along the guide rail. Between the two limit switch, the cavity can be investigated without dead ends. The rotation motor moving together with the cavity controls the photographing angle through a rubber belt. The camera pointer facing to the camera assists to find the right position where contains the defect.

In order to keep the characteristic of compact, the mini stepper motor PDx-108-28-SE-485 is the best choice, thanks to its small dimension (see Figure 4.5) and the small module of controller/driver electronics (see Figure 4.6) which are mounted to the back of the motor. This module converts the motor into a compact mechatronic device with serial bus oriented or standalone control.

The step angle is 1.8 °, and operating voltage is DC 24V. The encoder (the sensor IC is placed on the bottom of the PCB) measures the pole position and the angle and speed of the motor. The connection between the board and the desktop or laptop is based on RS485, which Supports multipoint communication.

The host (computer) controls the slave devices by broadcasting, the slave device (the motor) responses only the relevant instruction contains its own address code, other slave devices and the host remain silent during this responses. The slave device sends the finishing signal to the host after executing relevant instructions, then the host continues to execute the next instruction.

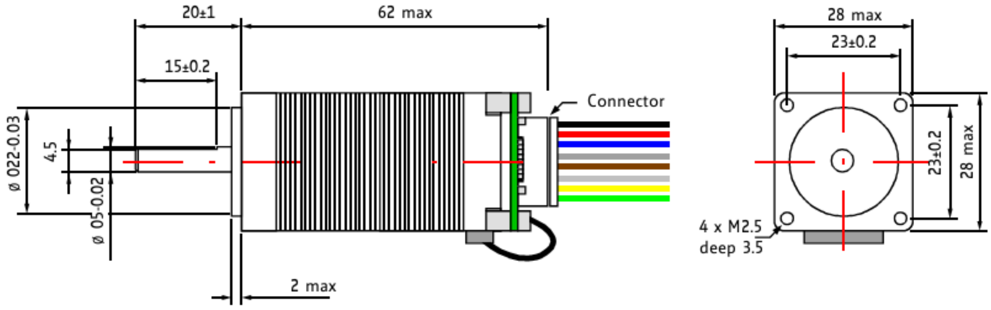

Figure 4.5 The dimension of the mini stepper motor (all values in mm).

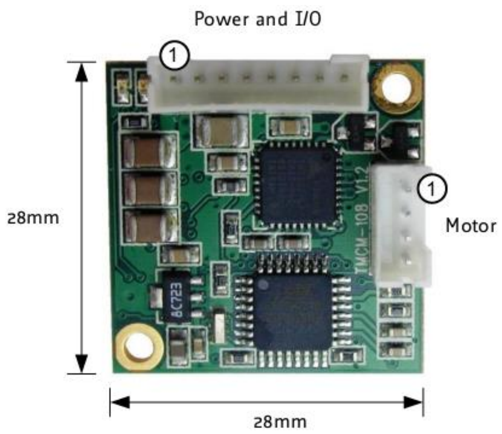

Figure 4.6 Top side of the board with connectors

The optical inspection system after updating is reported in Figure 4.7, and the power supply of the motor and the RS485-USB adapter are kept in a small box (Figure 4.8).

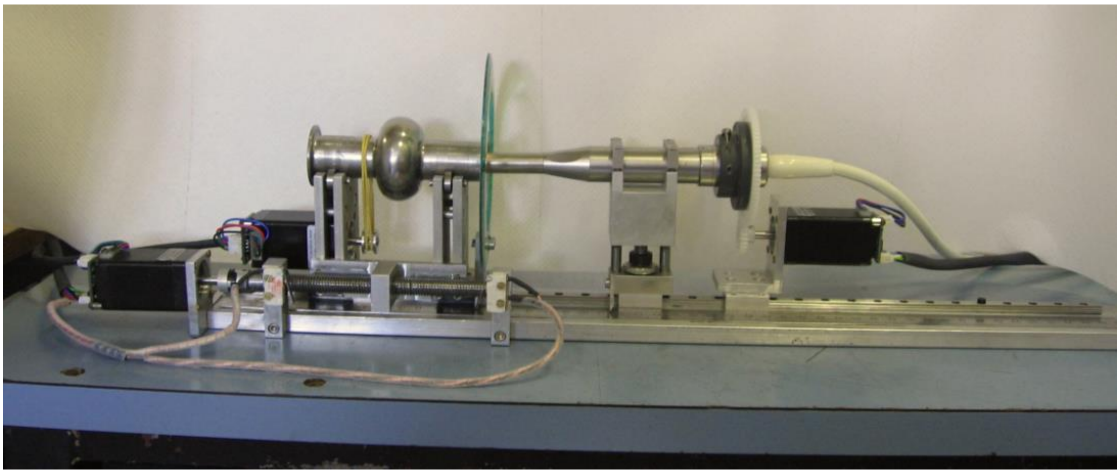

Figure 4.7 The optical inspection system after updating

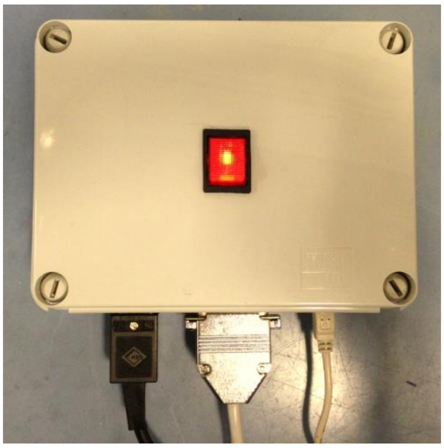

Figure 4.8 Power supply and motor connection box

4.2.2 Design of Software

Development of PC software consists of two parts, the first part is the three motor control, and the second part is the camera and photo management. All functions are implemented through LabVIEW.

1) Introduction of LabVIEW

LabVIEW (short for Laboratory Virtual Instrumentation Engineering Workbench) is a platform and development environment for a visual programming language from National Instruments. The graphical language is named "G". LabVIEW is commonly used for data acquisition, instrument control, and industrial automation on a variety of platforms including Microsoft Windows, various flavors of UNIX, Linux, and Mac OS X.

LabVIEW programs/subroutines are called virtual instruments (VIs). Each VI has three components: a block diagram, a front panel, and a connector panel.

One benefit of LabVIEW over other development environments is the extensive support for accessing instrumentation hardware. Drivers and abstraction layers for many different types of instruments and buses are included or are available for inclusion. These present themselves as graphical nodes. The abstraction layers offer standard software interfaces to communicate with hardware devices. The provided driver interfaces save program development time. Therefore, even people with limited coding experience can write programs and deploy test solutions in a reduced time frame when compared to more conventional or competing systems.

Using the LabVIEW, one new control system was built, the operation interface is presented in Figure 4.9. The left part is the real time video of the inner surface of the cavity, while the right-up part displays the caputered image. In the right top show the connection state of the motor and camera. In the right bottom half of the panel is the cavities information input elements and motor control functions which will be explained in the following.

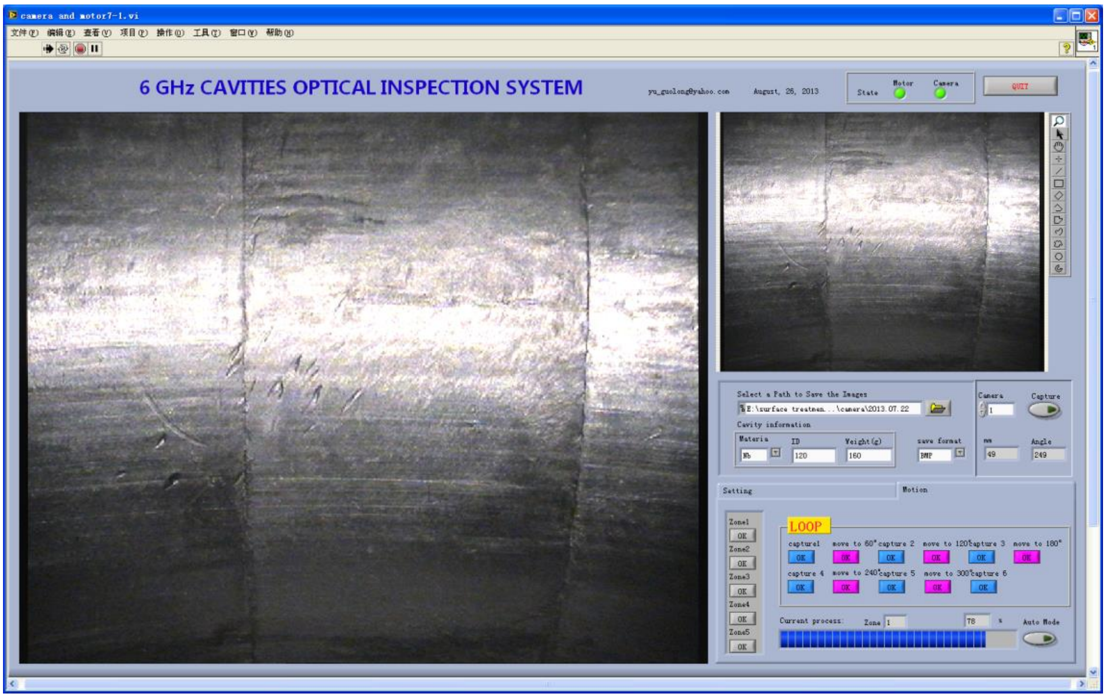

Figure 4.9 The operation interface of 6 GHz cavities optical inspection is developed using LabVIEW

2) Image Capture and save

Before taking the images, the operator should select a path to save them and input the cavity information, such as material of the cavity, cavity ID, weight and the format of the image, then the soft will save the images automatically, take the situation in the Figure 4.10 for example, to the path “..\Nb120\160g\19mm_0degreen” after execution of the capture, in which “19mm” is the length of cavity from the right, “0degreen” is the longitude angle.

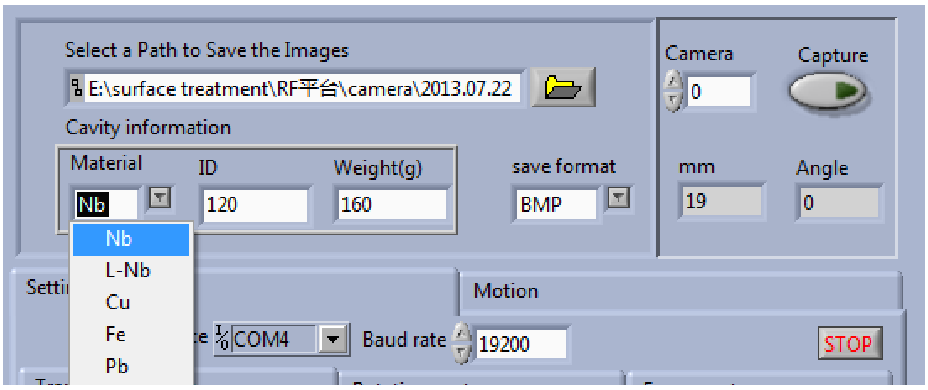

Figure 4.10 Front panel of image capture and save function

Figure 4.11 is the block diagram of image capture and save function, which is compose of camera scanning, open camera, configure and create images, capture and save images.

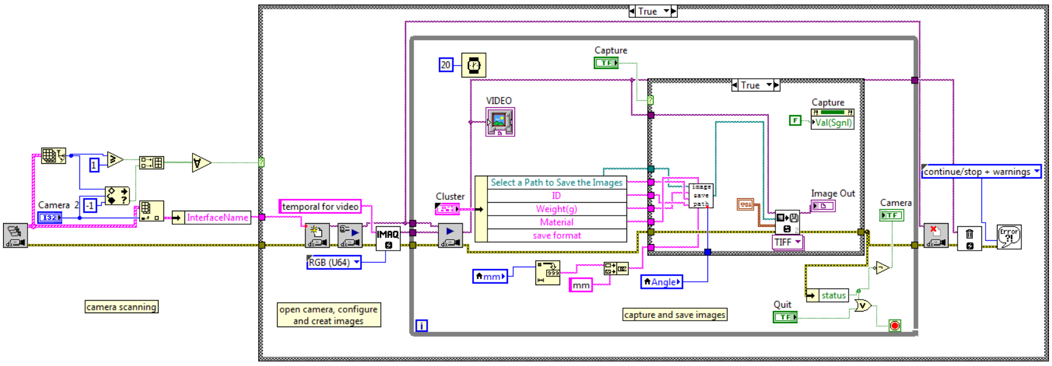

Figure 4.11 Block diagram of image capture and save function

3) Motor control

The motor controlling is made of tab controls. The setting page contains the interface parameter and the manual setting of three motors. In the motion page is the motor move and image capture activities.

Every command sent to the motor is used the sub-function “TMCL_sub.vi”, which was shown in Figure 4.12.

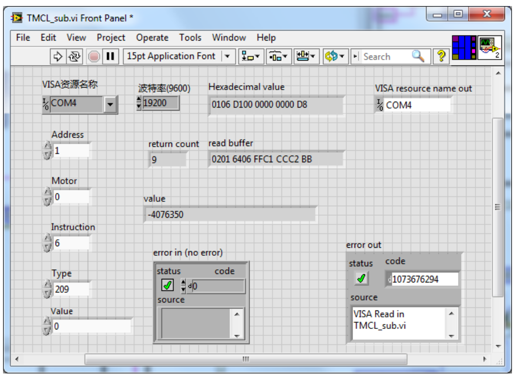

(a)

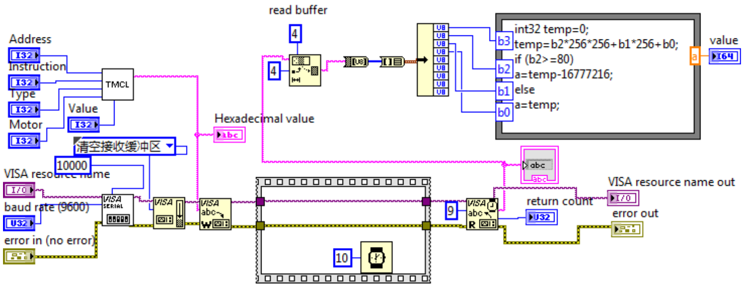

(b)

Figure 4.12 The front panel (a) and the block diagram (b) of the TMCL_sub.vi

In the block diagram of setting page, every motor commands are send by the “event structure” (Figure 4.13), while in the motion page, the commands are send by message queue (Figure 4.14).

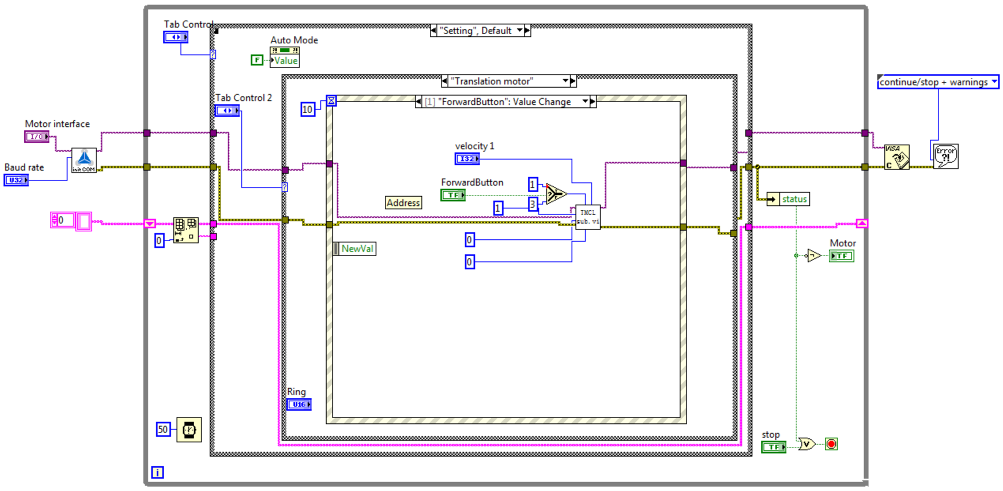

Figure 4.13 One instance of setting page

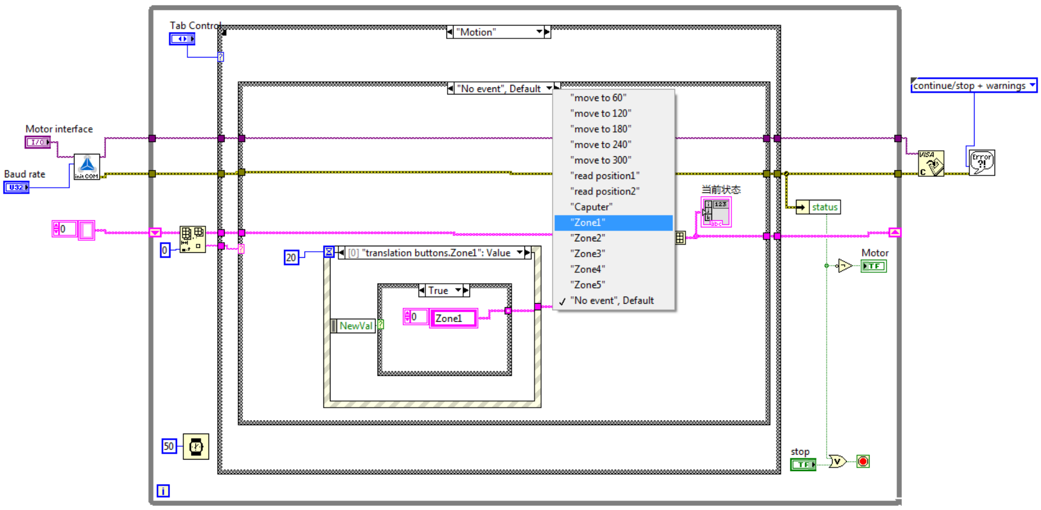

Figure 4.14 Commands in the motion page are send by message queue

a) translation motor

In this panel, the operator can move the cavity forward and backward along the guide rail and set 5 zones that he wants to investigate, the blue vernier shows the camera position, which is zero when cavity move to the left limit switch (Figure 4.15).

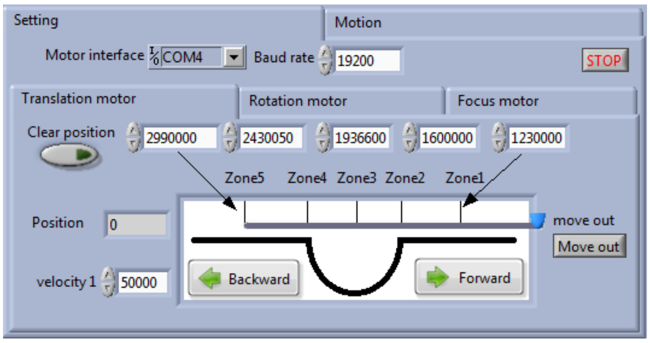

Figure 4.15 Translation motor control panel

b) rotation motor

At each zone of the cavity, 6 images are captured. In this rotation motor panel one should calibrate the position versus angle using the goniometer.

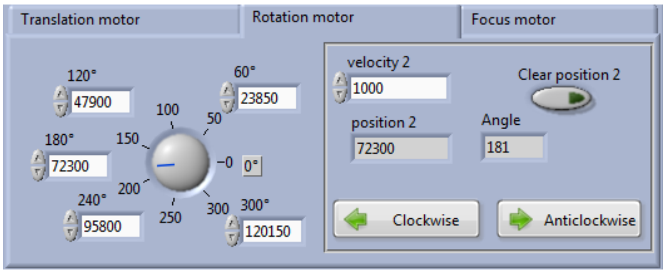

Figure 4. 16 Rotation motor control panel

c) focus motor

Due to the symmetry of the cavity, only 3 focus position should be set. Note that there is no limit switch for the focus motor, so be careful and watch the position in the panel when press zoom in or zoom out button. Otherwise, the focus function of the camera may be damaged.

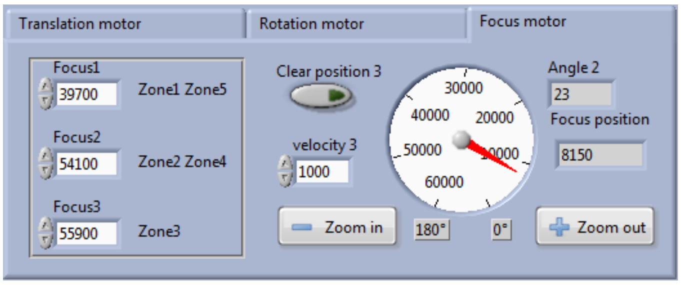

Figure 4.17 Focus motor control panel

d) manual and auto capture

After setting every motor in the desired position, the operator can capture the images step by step pressing every button in order or press the “Auto Mode” button only and just leave the computer to execute the whole process (Figure 4.18 and Figure 4.19).

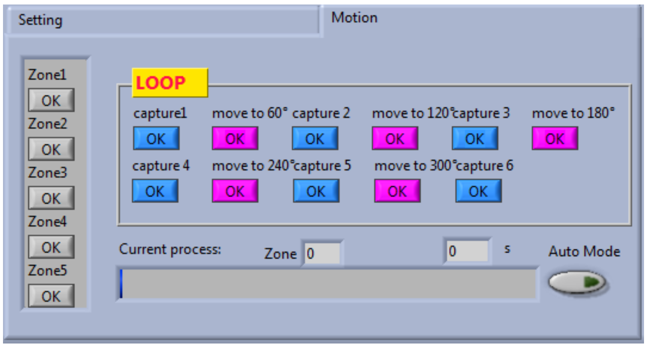

Figure 4.18 Manual and auto capture control panel

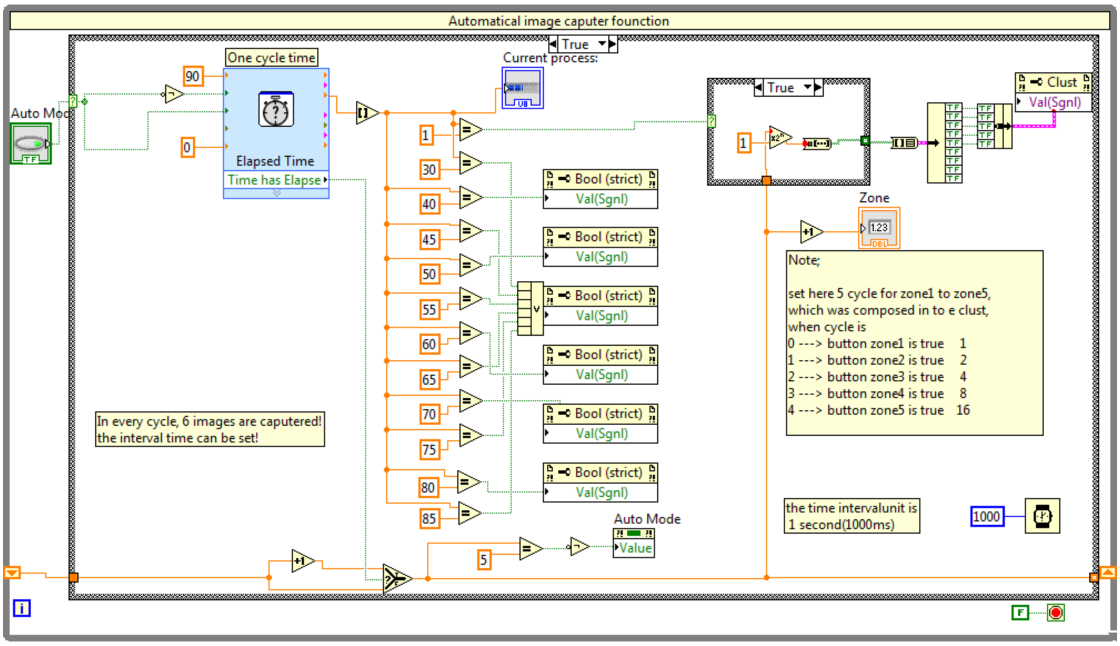

Figure 4.19 The block diagram of the auto mode function

Chapter 5

Results

We developed a new mechanical surface treatment for the internal finishing of 6 GHz superconducting cavities. It utilizes the principle of resonance of the spring with the vibrator to polish the inner surface of cavities, pushing the erosion efficiency to a new level, which is surpassing the CBP polishing efficiency.

In the research and development process, a complete set of mechanical polishing process was explored. Influences of abrasive materials type, quantity and mixing ratio, tumbling time, spatial arrangement of the vibrator on the polishing efficiency are discussed. It also compared the polishing efficiency of single cavity and that of multi-cavities using the same system.

5.1 Mechanical polishing process

5.1.1 Ultrasonic cleaning

Ultrasonic cleaning is the process of ultrasound in the liquid using cavitation effects, the acceleration effect, and straight flow effect to the liquids and dirt directly or indirectly, which makes the dirt layer disperse, emulsify, peel and achieves the purpose of cleaning.

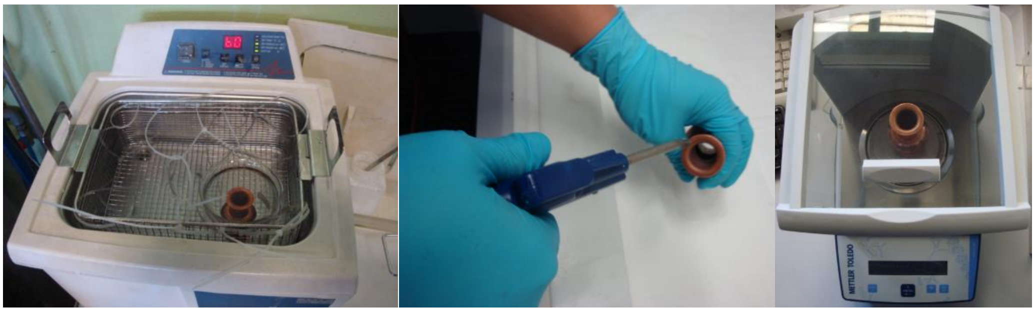

(a) (b) (c)

Figure 5.1 Preparation before tumbling: (a) Ultrasonic cleaning; (b) dry with nitrogen after rinsing with ethanol and acetone; (c) weight by electronic balance.

The ultrasonic cleaning is a physical cleaning technology, which frequency is above 20 kHz. It simplifies many traditional cleaning process and greatly improves the cleaning quality and production efficiency.

Ultrasonic cleaning aims at degreasing as the first step after the cavity being manufactured from the factory and proposes to removal residual media and material attaching to the inner surface of the cavity after each tumbling. The temperature is 60℃ and wash time is 1 hour. After ultrasonic cleaning, the cavity is needed to rinse with ethanol and acetone, dry with nitrogen gun, weight by electronic balance (reported in Figure 5.1).

5.1.2 Media selecting

In the vibrating process the cavity is filled approximately 50% by volume with a mixture of different media. The media is typically used with water and liquid soap to cool the cavity and remove material from the surface to allow for further polishing.

Media selecting is the most difficult part to achieving the final desired properties of the niobium surface. The fact that the exact condition needed or desired for the niobium surface is not known presents additional challenges.

Figure 5.2 shows three different types of abrasive media used in INFN-LNL. Small SiC triangular shaped blocks are extensively used in mechanical polishing, it is a very aggressive ceramic media and it can be used for the first low level mechanical polishing.5 mm sphere of zirconium dioxide is a high density material and can be used for the intermediate smoothing. Al_2O_3 plus SiO_2 (in PET) flakes are soft and can be used for the final surface finishing.

1 - SiC, 2 - ZrO_2.

Figure 5.2 Three different types of abrasive media.

5.1.3 Cavity mounting and polishing

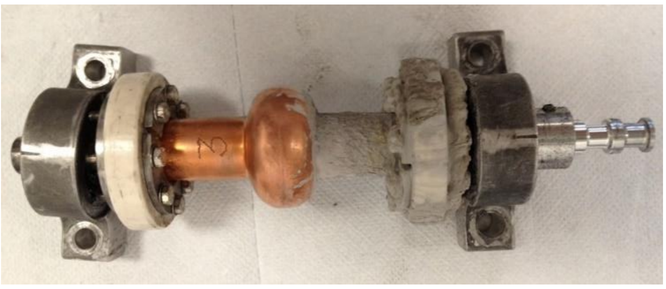

Figure 5.3 Leakage occurs on the not sealed well cavity during vibration

As shown in Figure 3.7, the cavity should be sealed up in both sides with the plastic blind flange. Since the mechanical polishing is a process of electric energy converted to mechanical energy, and part of mechanical energy is converted into heat. As the vibration goes on, the temperature of the cavity with the grinding fluid will rise, the volume of the internal gas expands, the muddy thing will erupt out as shown in Figure 5.3 if the O-ring is forgotten even the cavity close tightly.

The physical vibrating system is reported in Figure 5.4, the processes of how to start and stop vibrating is following,

a) It is necessary to check whether the vibrator is fixed with the spring washer which is very important for defending nut loosing before mounted cavities to the vibration system

b) The well-sealed signal or two or three cavities are then mounted to the vibration system by bolts. Make sure that the cavity can rotate itself freely after triggering by hand.

c) Modify the position of the motor to ensure the cavity rotation axis and the motor driven shaft to form belt cooperate.

d) Connect cavities and the motor with rubber belts, which are different length and may need to change a new one after several runs.

e) Power on the control box, the stepper motors start to sun, check if the cavities can rotate smoothly and the rubber belts can run in the slot rather than run out.

f) Set a low frequency, usually 60Hz in the control panel (Figure 5.5), and press the run key, alter the frequency until the noise comes from the cavity inside is big enough, which means the media grinding the cavity forcefully at high speed.

g) Check the polishing processing every half an hour if it work properly or not, and one can stop the system just pushing the stop key in the control panel if want to investigate the treatment result .

h) Disconnect the rubber belt, and detach the cavity from the plate.

i) Open the cavity and clean.

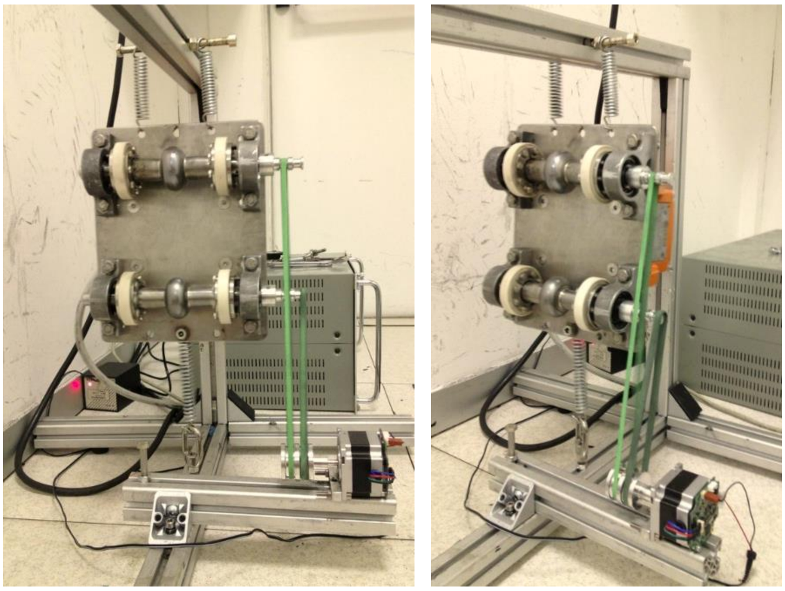

Figure 5.4 Picture of physical vibrating system

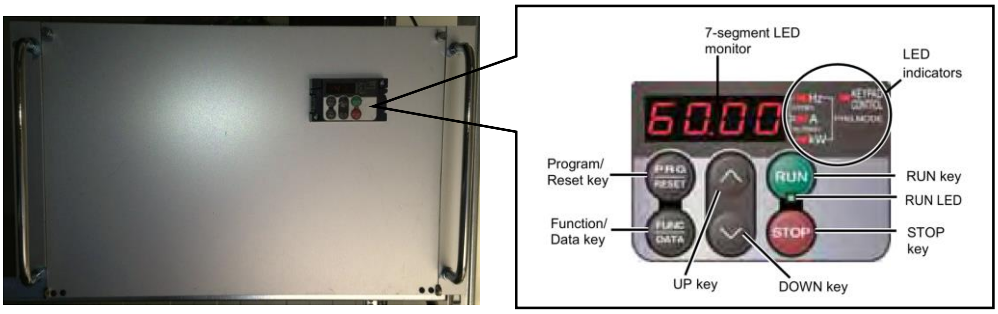

Figure 5.5 the control panel

5.2 The statistics of cavity tumbling

5.2.1 Different material cavities

Till now, eighteen 6 GHz cavities shown in Table 5.1 have been polished by vibrator, including eight 3mm and three 2mm thickness (which cavity ID with "L") Niobium cavities, 4 Ion cavities and 3 Copper cavities. The comparison of the inner surface condition before and after polishing are displayed in the Table 5.2.

Table 5.1 The statistics of cavity tumbling

Material	Cavity ID	Initial weight [g]	Final weight [g]	Total removed [g]	Tumbling time (h)
Niobium	Nb127	191.352	181.378	9.974	305
	Nb128	177.775	167.365	10.41	380
	Nb129	184.483	174.05	10.433	353
	Nb130	170.209	159.937	10.272	101
	Nb131	175.812	165.686	10.126	59
	Nb132	167.89	157.82	10.07	35.5
	Nb133	174.381	164.83	9.551	100.5
	Nb134	168.378	157.964	10.414	69.13
Iron	Fe1	149.576	144.316	5.26	66
	Fe2	141.112	134.368	6.744	66.1
	Fe3	142.8	135.253	7.547	95.6
	Fe4	154.431	145.828	8.603	98
Niobium	Nb-L148	119.26	110.919	8.341	81.05
	Nb-L149	112.923	105.509	7.414	70.09
	Nb-L150	117.073	109.795	7.278	70.09
Copper	Cu1	151.139	145.567	5.572	137
	Cu2	166.285	158.845	7.44	481.5
	Cu3	179.9	175.921	3.979	5.45

Table 5.2 The images of inner surface for different material cavities before and after tumbling

Nb	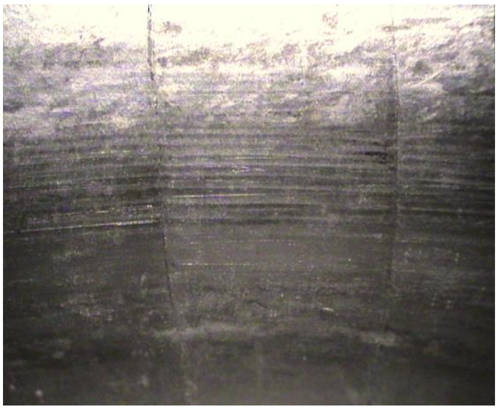	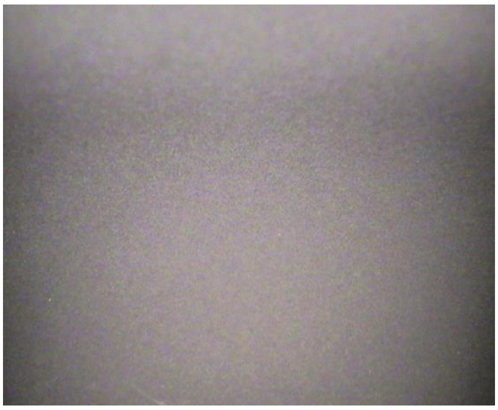
Fe	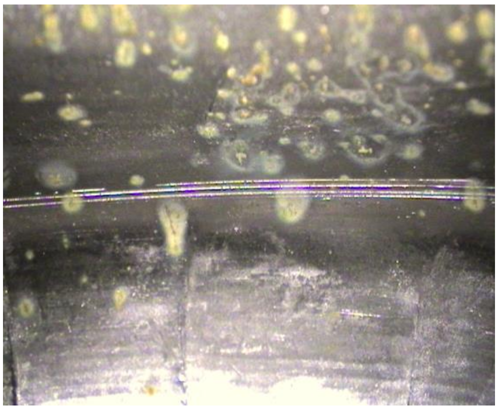	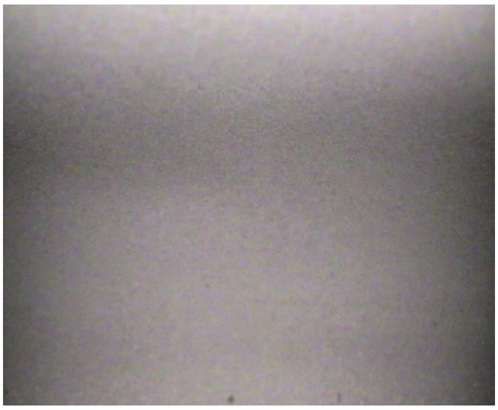
CU	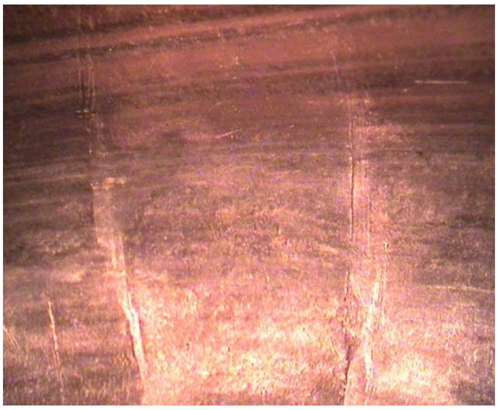	
material	Before tumbling	After tumbling

5.2.2 The highest erosion rate till now

The latest experiment result with Copper cavity Cu3: Erosion rate of 1 gram/hour was reached(as shown in Figure 5.6), which means 13 microns depth of inner surface materials was removed per hour (the Nb Density is 8.57g/cm3, and the area of inner surface of 6 GHz is 88 cm^2). The erosion rate decreased with the time, but in Run 3 the media must be blocked a while which cause the erosion rate smaller than Run 2.

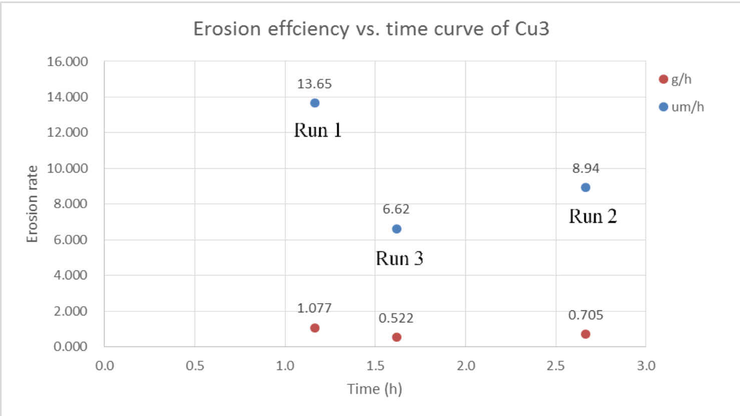

Figure 5.6 The latest tumbling result with Cu3 cavity

5.3 The RF test result

After treated by the standard surface polishing techniques which started from the new mechanical polishing, the cavity is experienced once or several UHV (ultra-high vacuum) annealing, and characterized by the cryogenic RF test eventually.

The RF test result (Figure 5.7) proves the effectiveness of the vibration therapy.

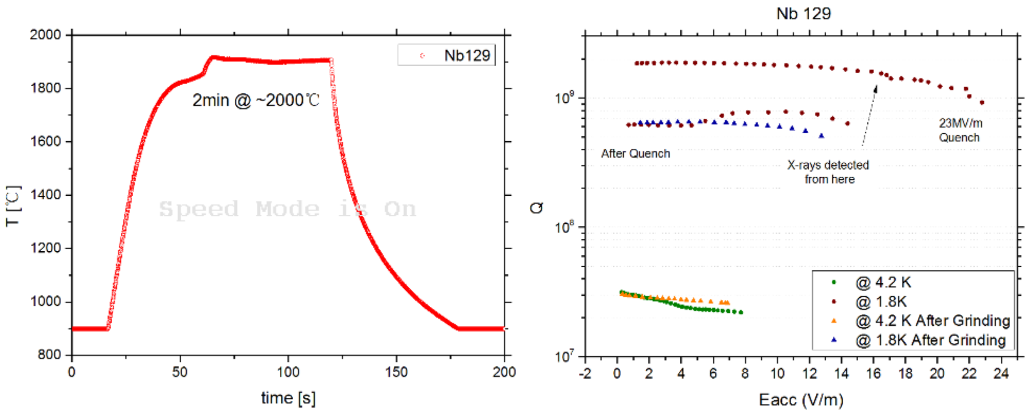

(a) (b)

Figure 5.7 (a) the annealing cycle after tumbling and EP. (b) Q-factor versus accelerating field at 4.2K and 1.8K after mechanical polished by vibration.

5.4 Discussion

5.4.1 Effect of tumbling time

SiC stone getting smaller, and angular shape (shown in Figure 5.8) gradually been polished to a smaller ball with the grinding time, not only the impact force reduce, but also the resulting powder with water to form a mixture, and these mixtures will hinder emery friction with the cavity, so the polishing effect will be getting worse.

However, short time grinding means frequent disassembly and assembly, will increase the manpower time, so it is very important to control the grinding time reasonably.

Figure 5.8 The new media and the used media (SiC)

Figure 5.9 shows the curve of erosion efficiency vs. time.

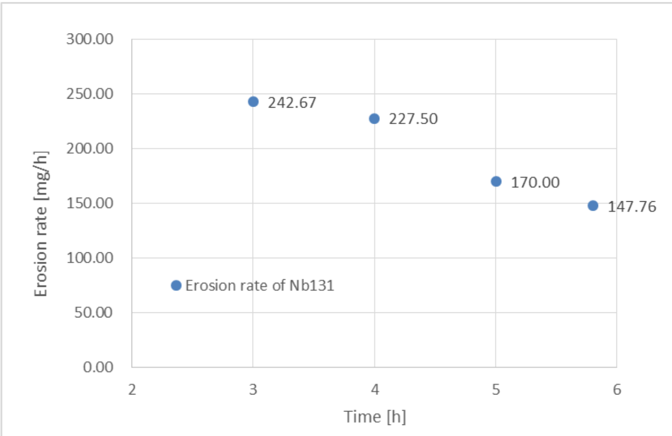

Figure 5.9 The erosion rate versus tumbling time.

5.4.2 Effect of media

In order to study the media effect on the erosion rate, the cavity Nb130 was tumbled with different number of media in each run (Figure 5.10), in which the tumbling time is the same (3 hours). The erosion rate reach the maximum value (above 300mg/h) when the cavity filled with 18 new SiC media while other conditions were the same. And it also shows that the Zirconia balls have no contribution to the erosion rate by comparison of run 2 and run 3, but it may be useful for polishing inner surface.

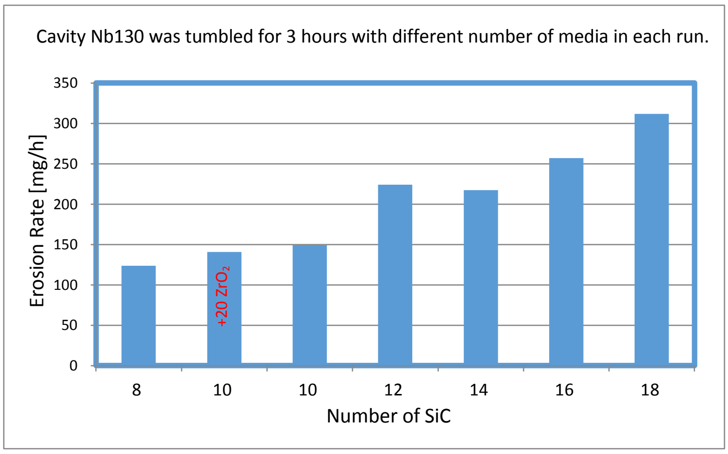

Figure 5.10 The erosion rate versus number of SiC

Usually, it is better to fill the cavity with some new media and some used media (SiC) together, which may increase the valid contact area and also ensure the enough polishing force.

5.4.3 Single and multi-cavities tumbling

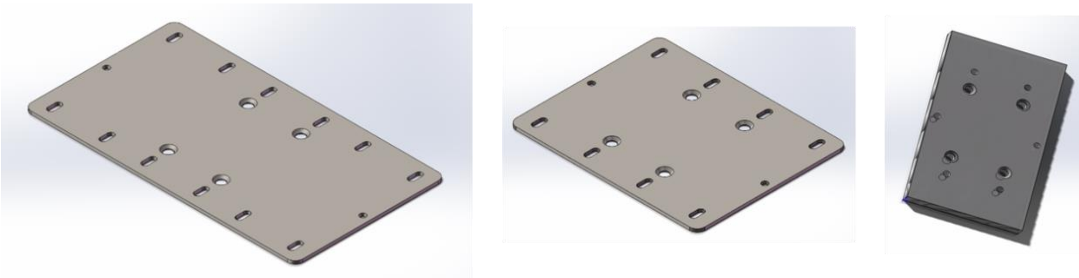

(a) (b) (c)

Figure 5.11 Different plate used in the polishing processes. (a) Triple cavities plate; (b) double cavities plate; (c) signal cavities plate.

Is it possible to polish more cavities in one run? The answer is sure. Using different size plate (Figure 5.11), signal, double and triple cavities can be tumbled in one run. But the vibration frequency will be a little bit different, because the load of the spring i.e. the total mass of the cavities and the vibrator are changed, the reason of which is explained in section 3.2.

Another different point is that it will cost double or triple time to dismount and mount, open and close two or three cavities in one run. However, in the same condition the result may be the one we expected, the erosion rate for each cavities in one run is not the same in the signal cavity tumbling (the erosion rate was 378mg/h in 3 hours) while just the total erosion rate is slightly higher than that in the later. It is clear in the Table 5.3 and Table 5.4. So it can induce that the conversion of electrical power to total mechanical power is nearly the same in three configuration, no matter how many cavities are tumbled in one run.

Table 5.3 The erosion rate in double cavity tumbling

Run		Top	Down	Total
1	Cavity ID	Nb129	Nb130	
(3hrs)	Erosion rate [mg/h]	213.33	224.33	437
2	Cavity ID	Nb127	Nb134	
(6hrs)	Erosion rate [mg/h]	120.83	154.5	275.33
3	Cavity ID	Nb129	Nb130	
(3.5hrs)	Erosion rate [mg/h]	216.86	177.43	394.29

Table 5.4 The erosion rate in triple cavity tumbling

Run		Top	Middle	Down	Total
1	Cavity ID	Nb128	Nb130	Nb127	
(3hrs)	Erosion rate [mg/h]	164.67	96.33	146.66	407.66
2	Cavity ID	Nb134	Nb129	Nb133	
(4hrs)	Erosion rate [mg/h]	185	43.25	176.25	404.5
3	Cavity ID	Nb128	Nb127	Nb130	
(3.5hrs)	Erosion rate [mg/h]	191.43	41	125.43	357.86
4	Cavity ID	Nb134	Nb133	Nb129	
(4.33hrs)	Erosion rate [mg/h]	189.61	*[1]	137.64	327.25+
5	Cavity ID	Nb127	Nb133	Nb128	
(17.75hrs)	Erosion rate [mg/h]	89.74	28.82	77.63	196.19
6	Cavity ID	Nb134	Nb129	Nb130	
(6hrs)	Erosion rate [mg/h]	217.5	32.83	159.5	409.83
7	Cavity ID	Nb127	Nb133	Nb128	
(15hrs)	Erosion rate [mg/h]	84.6	50.67	69.4	204.67

5.4.4 Effect of plate direction

In order to study the effect of plate direction on the erosion rate, the triple cavity vibration system was taken into experiment. The configuration was shown in Figure 5.12 and the result is reported in the Table 5.5. The system worked around 185 Hz at its own frequency the noise is highest. And the tumbling time is 4 hours.

The erosion rate for each cavity in vertical run is lower than that in the signal cavity tumbling; the erosion rate of the cavity in the middle is one third of that at top or down one due to its vibration amplitude is smallest among the three cavity; the total erosion rate in the horizontal condition is the lowest (see Figure 5.13) for the vibrator have to overcome the gravity of its own and the cavities and loss half of the mechanical power converted from the electrical power.

[1] * The cavity here at this run was not opened and gone on next vibration.

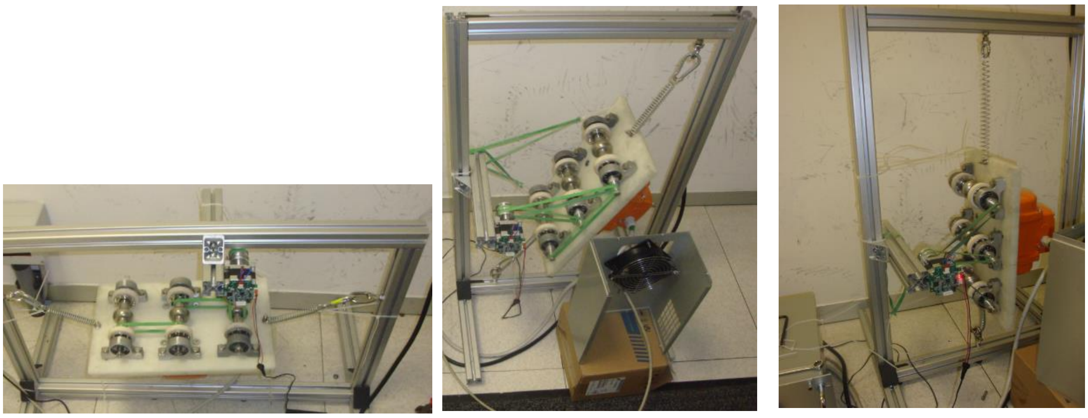

(a) (b) (c)

Figure 5.12 Triple cavity vibration system with three plate direction. (a) Horizontal; (b) Inclined (~60 °); (c) Vertical.

Table 5.5 The erosion rate of triple-cavity tumbling in different plate direction.

#Run	Sketch map	Processes				Total
1 (4h,190.7Hz)	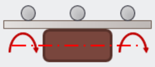	Cavity ID Left->right	Nb129	Nb130	Nb131	
		Erosion rate [mg/h]	80	48	48	176
2 (4h,186Hz)	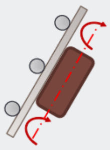	Cavity ID down->top	Nb130	Nb131	Nb129	
		Erosion rate [mg/h]	118.5	37.25	186	331.75
3 (9.25h,175Hz)		Cavity ID down->top	Nb128	Nb127	Nb132	
		Erosion rate [mg/h]	91.57	36	96.43	224
4 (4h,185Hz)		Cavity ID down->top	Nb133	Nb129	Nb134	
		Erosion rate [mg/h]	169.75	66.75	225.5	402
5 (4h,185Hz)	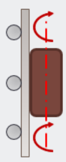	Cavity ID down->top	Nb128	Nb127	Nb132	
		Erosion rate [mg/h]	206.75	68	224	438.75
6 (4h,185Hz)		Cavity ID down->top	Nb133	Nb129	Nb134	
		Erosion rate [mg/h]	198.75	71.5	205.5	405.75

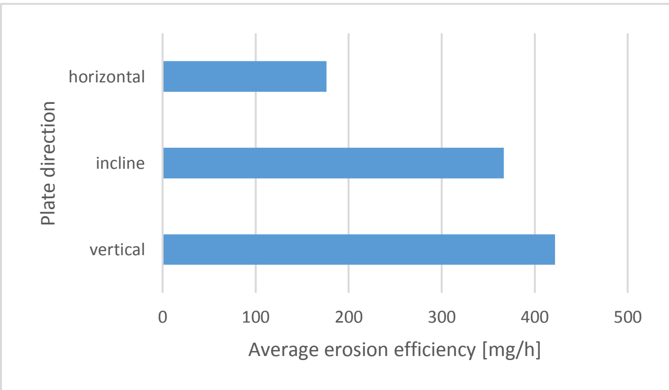

Figure 5.13 Erosion efficiency in different plate direction

5.5 Summery

After a lot of tests and analysis, we can sum up the experience of following,

1) Tumbling only one cavity in one run and stop it around 2 hours;
2) Like in the Figure 5.14, put some (~6) used (smaller) SiC in the bottom necklace and the new ones (~12) and (~20) ZrO_2 in the center, and put some(~6) used SiC again, fill deionized water up to the green line;
3) Shake the cavity by hand and feel that no block in it and then put it the vibration stand;
4) Fix the vibrator to the plate with screw and spring cushion;
5) Connect the springs up and down tightly and directly to the transom with less transition, and try to make the spring in vertical;
6) It is also useful to add 2 rubber belt up and down to ensure the balance during the shaking;
7) Set frequency around 200Hz. At this frequency it is very powerful for polishing but also to the bearings which should change when it work not well(can't rotate smooth), otherwise, it may block and it (polishing contain part overly) is very bad for the cavity
8) Every half hour, go and check the operating state.

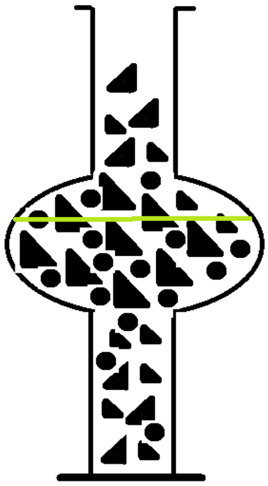

Figure 5.14 Diagram of the media filling into the cavity

Chapter 6

Conclusions and next plan

6.1 Mechanical polishing treatment for 6GHz cavities

Mechanical polishing bases on the resonance principle for 6GHz superconducting cavity of the inner surface finish is a new attempt, the results show that the method is effective.

A low cost, simple structure, convenient operation, and efficiency considerable mechanical polishing systems were developed as a result of carefully designed and systematic study.

Therefore, one cavity will be ready for next treatment in 20 hours' tumbling, after this short period of mechanical treatment, 10 grams of inner surface materials are removed and the bump indentations disappear, which satisfy our goal.

6.2 Idea for 1.3GHz mono-cell cavities vibration polishing system

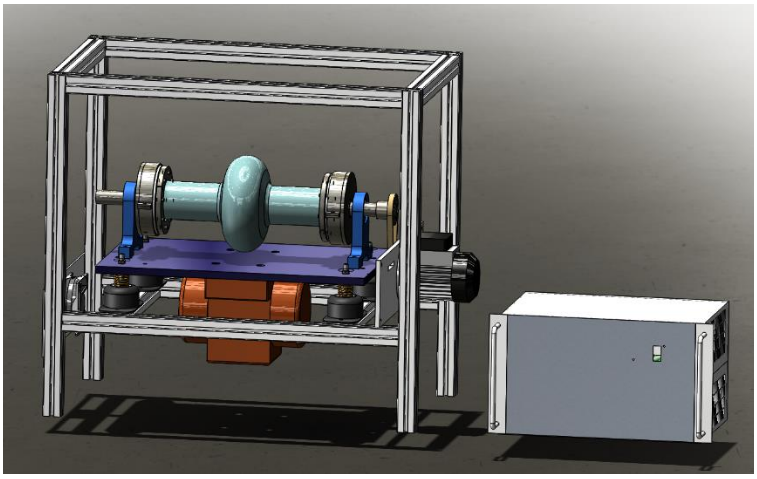

Figure 6.1 the conceived drawing of the 1.3GHz mono-cell cavities vibration polishing system

The idea of our design derives from the principle of vibrating screen, which is used for selection of the small matter from the mass.

The vibrator is placed horizontally as it is very difficult to balance the whole system if set in verticality as the same with the 6 GHz cavities vibrating system due to the heavy weight of vibrator and cavity; the springs and the shock absorber feet make the system stable. What's more, it is possible to find the best resonance frequency with different springs; it is convenient to mount and dismount the cavity without uninstalling the cavity holders, compared to previous integral design; the cavity is rotated by the belt, tightness of which is adjustable along with the vibrating using a spring.

Bibliography

[1] B. Anne, et al. Superconducting TESLA Cavities, Physical Review special Topics-Accelerators and Beams, Volume 3, 092001(2000).

[2] H. Padamsee, J. Knobloch, T. Hays, RF Superconductivity for Accelerators, John Wiley & Sons, Plenum Press, San Diego, 1998.

[3] TESLA, Technical Design Report, The Accelerator, Eds. R. Brinkmann, K. Flöttmann, J. Rossbach, P. Schmüser, N. Walker, H. Weise, DESY report 2001-23 (2001)

[4] International linear collider reference design report, ILC global design effort and worldwide study, August, 2007

[5] D. Proch, P. Schmueser, W. Singer, et al., Niobium in superconducting RF cavities, Niobium 2001 International Symposium, DEC 02-05, 2001 Orlando, Florida, USA

[6] P. Schmüser, "Basic principles of RF superconductivity and superconducting cavities", Workshop 'Pushing the Limits of RF Superconductivity', September 22-24, Argon National Laboratory, USA, 2004

A. Matheisen, "Improvements on standard Fabrication methods", ibid ref. 5

[7] J. Brawley, J. Mammosser, L. Phillips, "Electron beam weld parameter development and cavity production costs", Proceedings of the 1997 Workshop on RF Superconductivity.

[8] V. Palmieri "Seamless Cavities: the most creative topic in RF Superconductivity," 8th Workshop on RF Superconductivity, Abano Terme (Italy), October 1999.

[9] V. Palmieri, "Advancements on spinning of seamless multi-cell reentrant cavities", Proc of the 11th Workshop on RF Superconductivity SRF2003.8-12 September 2003, Luebeck, Germany, TuP26.

[10] P. Kneisel, V. Palmieri, K. Saito, "Development of Seamless Niobium Cavities for Accelerator Application", Proceedings of the 1999 IEEE Particle Accelerator Conference. 29 Mar - 2 Apr 1999, New York, New York. 18th IEEE Particle Accelerator Conference, p.943-945

[11] L. Badan, C. Durand, V. Palmieri, R. Preciso, S. Stark, F. Stivanello, W. Venturini, "R.F. characterization of small scale cavities", Proceedings of the 1997 Workshop on RF Superconductivity, Abano Terme (Padova), Italy

[12] V. Palmieri, "Spinning of TESLA-Type Cavities: Status of Art"., Proc. of the 9th Workshop on RF superconductivity, Santa Fe, USA, Nov. 1999, pp 532-537.

[13] V. Palmieri, R. Preciso, V.L. Ruzinov, S.Yu. Stark, S. Gambalonga, Forming of seamless high beta accelerating cavities By the spinning technique, Nuclear Instruments and Methods in PhysicsResearchA342(1994)353-356,North-Holland

[14] D. Bloess, “Chemistry and Surface Treatment”, SRF-84, Geneva, July 1984, Proceedings pp. 409-425.
[15] K. Saito et al., “Superiority of Electropolishing over Chemical Polishing on High Gradients” SRF-97, Italy, October 1997, Proceedings pp. 795-813.
[16] Michigan State University internal note.
[17] TESLA Technical Design Report R. Brinkmann, et al., Editors. 2001, DESY: Hamburg.
[18] http://www.glenmills.com/powder-blending/turbula-shaker-mixer/
[19] C. Cooper et al., “Centrifugal Barrel Polishing of Cavities Worldwide”, 15th International Conf. on RF Supercond., Chicago, IL (2011) WEIOA02.
[20] http://en.wikipedia.org/wiki/Vibrator_(mechanical)
[21] Siskind, Charles S. (1963). Electrical Control Systems in Industry. New York: McGraw-Hill, Inc. p. 224.ISBN 0-07-057746-3.
[22] https://en.wikipedia.org/wiki/File:VFD_System.png.
[23] http://www.acu-vib.com.au/accelerometers.htm

List of Figures

Figure 1.1 A TESLA nine-cell 1.3 GHz superconducting niobium cavity [4]. 3
Figure 1.2 Measured surface resistance of a 9-cell TESLA cavity. The residual... 4
Figure 1.3 General fabrication steps of standard fabrication technique for s.c. Cavities 5
Figure 1.4 Spinning of a seamless mono-cell resonator from a circular blank. No intermediate annealing is required during forming. 8
Figure 1.5 Process comparison of conventional and seamless cavity Fabrication 9
Figure 1.6 Picture of 6 GHz cavities made by different material. From left to right are Niobium cavity (thickness 3mm), lighten Niobium cavity (thickness 2mm), Cooper cavity, Iron cavity and Lead cavity. 10
Figure 1.7 The 6 GHz cavity geometry 11
Figure 1.8 (a)Drawings of the die, which is composed of two cylinders and a shell, assembled and ready for the spinning operation; (b)Disassembled when partially extracted after spinning; (c)Exploded view of the nylon shell of the die with all its ten sectors. 11
Figure 1.9 Image of inner surface at the center of the cavity, two evident vertical scratches shown in the red rectangles.. 12
Figure 1.10 Metallographic polishing machine with sandpaper 13
Figure 1.11 The stand for BCP and EP.. 13
Figure 1.12 The schematic diagram of EP 14
Figure 1.13 HPR for 6 GHz cavities in LNL-INF.. 14

Figure 2.1 TURBULA® Shaker-Mixer (model T2F) and 6 GHz cavity 15
Figure 2.2 The section of the configuration of cavity before mounting to the TURBULA® Shaker-Mixer 16
Figure 2.3 Schematic diagram of the Centrifugal barrel polishing (CBP). The red point is the reference point when the angular velocity of the barrel related to the turntable $\omega 2$ equals to zero. 17
Figure 2.4 (a) Photograph of the CBP system in INFN-LNL. (b) The configuration of the cavities. 18
Figure 2.5 Industrial centrifugal barrel polishing machine 18
Figure 2.6: Schematic of main shaft and 2 barrels of a centrifugal barrel polishing machine denoting the directions of rotation. This is a model of the Fermilab machine with a 9-cell Tesla – type cavity and counterweight shown in the barrels 18

Figure 2.7 The 3D drawing (a) and entity (b) of the zigzag tumbler 19
Figure 2.8 Polishing brush on the market 20
Figure 2.9 3D drawings of “flower brush”. 20
Figure 2.10 Photograph of “flower brush”. 20
Figure 2.11 Abrasive material. (a) Sand paper; (b) Scotch Brite 21
Figure 2.12 “flower brush” with abrasive material. 21
Figure 2.13 The way of putting “flower brush” into the cavity. 22
Figure 2.14 The “flower brush” was polishing the cavity on the lathe. 22
Figure 2.15 The petals were spreading in high rotating speed 22
Figure 2.16 Polish the inner surface of cavity by pneumatic hand held polisher using “flower brush”. 23

Figure 3.1 The configuration of combined spring vibration system 26
Figure 3.2 Picture of the firstly using vibrator 28
Figure 3.3 One example of the vibrator system for 6 GHz cavity 28
Figure 3.4 The diagrams of Assembly process before hanging up 28
Figure 3.5 A complete mechanical (Vibrator) process-cavity mounted on vibrator through PMMA-glass (15 mm thick) support plate (transparent in figure) . 29
Figure 3.6 Drawing of bearing holder and image of self-aligning bearing 30
Figure 3.7 Drawing of mechanical configuration of the cavity. The assembled state is at left, and the Exploded Views is at right. 30
Figure 3.8 Drawing of the belt axis 30
Figure 3.9 The internal structures images of one commercial vibrator 31
Figure 3.10 Images in first line is the consequence after neglecting the sponge, while in second line is the wright connecting way. (a) The cable was broken-down; (b) the cable was hurt by the shroud; (c) the cable was hurt by the cable jointing sleeve; (d) using the sponge to save the cable; (e) using electrical adhesive tape to protect the cable. 31
Figure 3.11 Sectional view of the inner and chassis dimensions 32
Figure 3.12 Diagram of the electrical connection 32
Figure 3.13 The main principle diagram of the VFD 32
Figure 3.14 Picture of real products FRN4.0E1S-4E which keypad can install to the front panel of the control unit of the vibrating system by the cable with RJ-45 connectors 33
Figure 3.15 3 phase RFI Filter 33
Figure 3.16 Schematic drawing of the vibrating system equipped with two 6 GHz cavities 34
Figure 3.17 connection of the spring and the plate using the custom nuts 35
Figure 3.18 Image of programmable stepper motor 35
Figure 3.19 Drawing of motor belt wheel 35
Figure 3.20 The cross section view of the accelerometer 36
Figure 3.21 The schematic diagram of impact sensor. 36

Figure 3.22 One example of the commercial impact sensor. 37
Figure 3.23 The drawing of the custom impact sensor 37
Figure 3.24 Schematic of the trigger capture and fault display circuit. 37
Figure 3.25 The connector circuit in the inventor. 38

Figure 4.1 The optical inspection equipment before updating 40
Figure 4.2 Photo software interface 40
Figure 4.3 The cross section of the 6 GHz cavity 41
Figure 4.4 3D schematic diagram of the optical inspection system mechanical upgrades 41
Figure 4.5 The dimension of the mini stepper motor (all values in mm). 42
Figure 4.6 Top side of the board with connectors 42
Figure 4.7 The optical inspection system after updating 43
Figure 4.8 Power supply and motor connection box 43
Figure 4.9 The operation interface of 6 GHz cavities optical inspection is developed using LabVIEW 44
Figure 4.10 Front panel of image capture and save function 45
Figure 4.11 Block diagram of image capture and save function 45
Figure 4.12 The front panel (a) and the block diagram (b) of the TMCL_sub.vi 46
Figure 4.13 One instance of setting page 46
Figure 4.14 Commands in the motion page are send by message queue 46
Figure 4.15 Translation motor control panel 47
Figure 4. 16 Rotation motor control panel 47
Figure 4.17 Focus motor control panel 47
Figure 4.18 Manual and auto capture control panel 48
Figure 4.19 The block diagram of the auto mode function 48

Figure 5.1 Preparation before tumbling: (a) Ultrasonic cleaning; (b) dry with nitrogen after rinsing with ethanol and acetone; (c) weight by electronic balance. 49
Figure 5.2 Three different types of abrasive media. 50
Figure 5.3 Leakage occurs on the not sealed well cavity during vibration 50
Figure 5.4 Picture of physical vibrating system 51
Figure 5.5 the control panel 52
Figure 5.6 The latest tumbling result with Cu3 cavity 54
Figure 5.7 (a) the annealing cycle after tumbling and EP. (b) Q-factor versus accelerating field at 4.2K and 1.8K after mechanical polished by vibration. 54
Figure 5.8 The new media and the used media (SiC) 55
Figure 5.9 The erosion rate versus tumbling time. 55
Figure 5.10 The erosion rate versus number of SiC 56
Figure 5.11 Different plate used in the polishing processes. (a) Triple cavities plate;

(b) double cavities plate; (c) signal cavities plate. 56
Figure 5.12 Triple cavity vibration system with three plate direction. (a) Horizontal; (b) Inclined (~60 °); (c) Vertical. 58
Figure 5.13 Erosion efficiency in different plate direction 58
Figure 5.14 Diagram of the media filling into the cavity 59

Figure 6.1 the conceived drawing of the 1.3GHz mono-cell cavities vibration polishing system 61

List of Tables

Table 5.1 The statistics of cavity tumbling 52
Table 5.2 The images of inner surface for different material cavities before and after tumbling 53
Table 5.3 The erosion rate in double cavity tumbling 57
Table 5.4 The erosion rate in triple cavity tumbling 57
Table 5.5 The erosion rate of triple-cavity tumbling in different plate direction. 58

Acknowledgements

First of all, I would like to extend my sincere gratitude to my supervisor, Prof. V. Palmieri, for his instructive advice and useful suggestions on my thesis. I am deeply grateful of his offering me the opportunity to learn this Master course. And in this academic year, he arranged our course with mature deliberation and taught us tirelessly, which let us grasp the theory also provided us with more opportunities to practice. All of these expanded my horizon and knowledge and my capacity of scholarship has been tested and benefited; thank him for his concern for me care for me in life, he is kind and humility, a scholarly mentor and beneficial friend; thank him providing me with a great convenience; thank him for his confidence in me, giving me the opportunity to play freely at work, I voracious sucked knowledge nutrition like a just born infant, and was fearless with difficulty like a newborn calf.

High tribute shall be paid to Ms. Silvia Martin, who provided me with all aspects of care and help, let me live and study in a foreign country without problems.

I am deeply indebted to my tutor, Antonio Rossi, who was my guide in terms of low-temperature superconductivity, I am impressed on his young and promising, modesty, kindness and helpfulness.

Special thanks should go to Alex, a young and powerful man, who gave me much support in my work. Without his help in the machining, my work would be difficult to make progress.

I also owe my sincere gratitude to thank Ram Krishna Thakur, who gave me a very big help in my work, and carefully guided me to understanding of daily laboratory operations step by step.

And I also want to thank all the other colleagues in the laboratory, the moments of working with them is destined to become a good memory my life.

I should finally like to express my gratitude to my beloved family, especially my mother-in-law, who is helping me to take good care my three years old son in Beijing during my abroad. I also owe my sincere gratitude to my lovely wife Yue Lin, whose understanding and supporting without a word of complaint motivated me to work hard.